5-2013

600 Years of Late Holocene Climate Variability Inferred from a Varved Proglacial Sediment Record Linnévatnet, Svalbard, Norway

Colin W. Dowey
Bates College, cdowey@bates.edu

Michael J. Retelle
Bates College, mretelle@bates.edu

600 Years of Late Holocene Climate Variability Inferred from a Varved Proglacial Sediment Record Linnévatnet, Svalbard, Norway

Bates College Geology Thesis

Presented to the Faculty of the Department of Geology, Bates College,
in partial fulfillment of the requirements for the Degree of Bachelor of Science

by
Colin W. Dowey

Lewiston, Maine
April 1st, 2013

Abstract

The varved proglacial sediment record preserved in Linnévatnet, Svalbard, Norway contains a valuable climate signal that can be used to reconstruct local Late Holocene climate variability. Two cores analyzed in this study, LH-4 and LH-Long were collected in May, 2012 from a distal location 1.5 km from the main inlet. This distal location allowed for a long record to be collected and the lack of sub-annual layers allowed for accurate measurement of varve thickness, the primary climate proxy. Through analysis of the Linnédalen proglacial system, and comparisons to the instrumental record it is clear that varve thickness is directly related to Linnéelva yearly sediment flux, Linnébreen mass balance, and summer temperature. Varve thickness and other potential climate proxy measurements were accurately placed back through time through the development of a plutonium-verified varve chronology. The varve chronology derived from counting and measuring yearly lamination couplets throughout core LH-4, is one of the highest resolution chronologies established in Linnévatnet.

From the interpretation of the Linnévatnet climate proxies and comparisons with other Svalbard paleoclimate reconstructions four periods of warm summer temperatures and four periods of cool summer temperatures in Linnédalen were projected. The warm periods, defined from AD pre-1379 to late 1390's, from AD 1760's-1790's, from AD 1850's to AD 1870's, from AD 1980's-present, relate to either steady increases in LH-4 varve thickness or intervals where varve thickness remains above average. The cool periods, defined from AD 1400-1450's, AD 1550's-1580's, AD 1790's-1850's and AD 1950's-1980's, relate to either steady decreases in LH-4 varve thickness or intervals where varve thickness remains below average. Further comparisons between the paleoclimate reconstruction presented in this study and regional-scale Late Holocene climate reconstructions indicate strong correlation between climate conditions in Linnédalen and NAO mode. This relationship confirms the influence of the NAO on the climate of western Spitsbergen.

Acknowledgments

First, I would like to thank the National Science Foundation, the Bates Student Research Fund and the Bates College Geology Department for providing funding that allowed for the completion of this project.

I would like to thanks William Ash and Mathieu Duvall for their help in the Imaging Center from scanning thin sections to formatting this document. Also, thank you to Greg Anderson for his time training me on the SEM microscope.

Thank you to all of the senior geology majors: David, Conor, Lauren, Rachel, Amanda G, Amanda W, Eric, Margaret, and Chester for keeping me company in Coram and helping me with every step in this process. From late night trips to the Den to night hikes in Whites during GSA, spending this year with you has been so wonderful.

I would like to thank Sarah Wason and my family for their help and their patience as they listened to me babble about this project. Sarah, thanks for helping me with my presentations as I repeated them for what must have felt like days and making me take breaks from the computer when my eyes were falling out. Thank you to my sister, mom, and dad for their support throughout this entire year with regard to with project and much more.

Finally, I am tremendously grateful to Mike Retelle for everything he has done throughout my time at Bates. Ever since seeing those first pictures of Svalbard in Sedimentology class I knew that it was somewhere that I would love to work. It was an honor to work closely with you this year on this project. Your enthusiasm for the Arctic is unparalleled and I like to think that some of that passion has rubbed off on me. Thank you for allowing me to work on such an interesting project even after summer field work and the Round Pond project didn't work out. This experience has been more than I ever could have hoped for and would not have been possible without your guidance.

Note to Reader

Many geographic features mentioned in this study are reffered to by their Norwegian names. Thus, Linnévatnet is Lake Linné, Linnédalen is the Linné Valley, Kapp Linné is Cape Linné, Linnébreen is the Linné Glacier, and Linnéelva is the Linné River.

Contents

List of Figures

List of Tables

Introduction

Purpose and Significance

Global climate systems have experienced unprecedented change over the last century due primarily to a severe increase in greenhouse gas concentrations (IPCC, 2007). The Arctic is particularly responsive to current climate change due its location and the presence of amplifying feedback loops. This sensitivity is indicated by increases in average Arctic temperatures of almost twice the global average over the past 100 years (IPCC, 2007). In order to place the current transformation of the Arctic into context and anticipate the effects of future climate change, Arctic climate change in the past must be quantified and understood (D'Andrea et al., 2012).

The purpose of this study is to reconstruct climate conditions in Western Spitsbergen, Svalbard, Norwegian High Arctic during the Late Holocene, on a yearly to decadal scale, from the sediment record preserved in proglacial lake Linnévatnet. The lacustrine sediments in Linnévatnet are closely tied to the growth and ablation of Linnébreen, an upstream polythermal cirque glacier (Svendsen and Mangerud, 1997). Due to the sensitivity of glaciers to changes in climate conditions the sediment record from Linnévatnet contains a climate signal back through time (Lowell, 2000).

The sediment record from Linnévatnet is comprised of annual lamination couplets called varves. The couplets are comprised of a summer layer and a winter layer. The constant periodicity of the lamination couplets allows the sediment record to act both as a climate proxy and a geochronometer. Previous studies have analyzed the physical characteristics of proglacial sediment records and related them to the timing of glacier growth and retreat within the watershed, and therefore changes in environmental parameters including temperature and precipitation (Leeman & Niessen, 1994; Mangerud and Svendsen, 1990; Snyder et al., 2000; D'Andrea et al., 2012).

Study Area

Svalbard is an archipelago located between 74°N and 81°N, and 10°E to 35°E, in the Arctic Ocean as indicated in Figure 1. Svalbard has an area of 61,020 km^2 and is 60% glaciated (Ingolfsson, 2006). The proglacial lake examined in this study, Linnévatnet, is located on Spitsbergen, the largest island in Svalbard. Linnévatnet resides within the valley, Linnédalen, on a small cape, Kapp Linné, located on the southern edge of Isfjorden, the largest fjord of Spitsbergen as indicated in Figure 2.

Linnévatnet is 4.7 km in length, 1.3 km in width and the long axis runs NNW-SSE. The lake surface lies at a height of 12 m asl and the northern end is 2 km from the Isfjorden margin (Svendsen et al., 1987). The primary inflow to Linnévatnet is meltwater from a polythermal cirque glacier, Linnébreen. The meltwater travels 6 km in a braided stream, Linnéleva, across a large outwash plain into the southern end of Linnévatnet. The north end of Linnévatnet drains into Isfjorden. The watershed of Linnévatnet is shown in red in Figure 3, a topographic map of Kapp Linné.

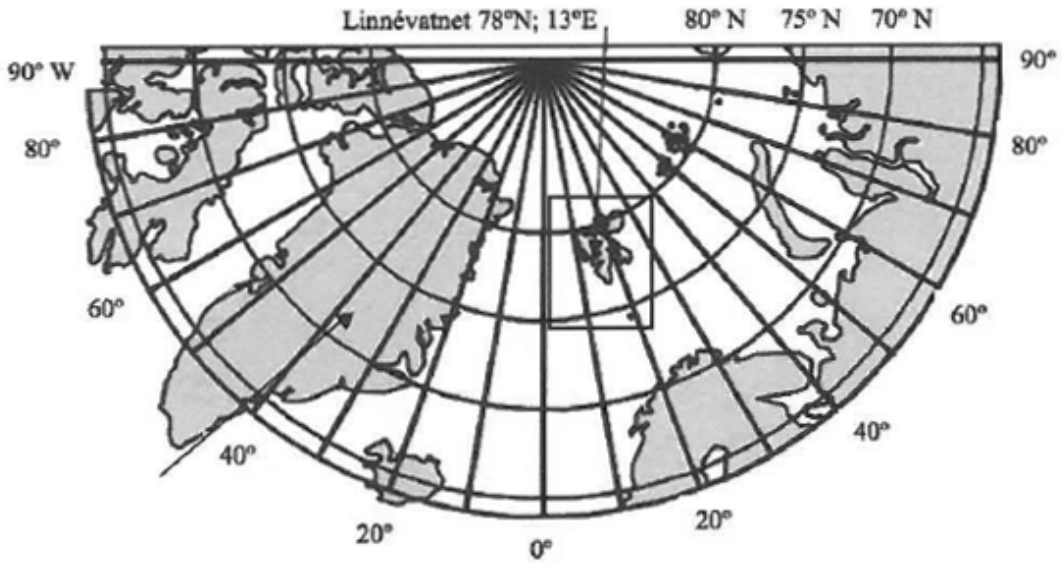

Figure 1 - A location map showing the location of Svalbard, indicated by the rectangle, between northern Greenland and northern Norway. The coordinates of Linnévatnet are shown above the map (Figure modified by Nelson, 2010 from Pomepani et al., 2009).

Figure 2 - A map of Svalbard showing the location of Longyearbyen, the most populous area, and Linnédalen, the field site for this study. Both locations are located along the southern edge of Isfjorden the largest fjord in Spitsbergen (Figure modified by Nelson, 2010 from Pomepani et al., 2009).

Figure 3 - A topographic map of Kapp Linné. Linnévatnet is the large lake to the north and Kongressvatnet is the smaller lake to the east. The watershed of Linnévatnet is indicated in red. (Figure modified by Nelson, 2010 from Motley, 2006)

The southern kilometer of the lake contains two sub-basins divided by a N-S trending ridge. The eastern sub-basin receives sediment from Linnéelva while the western sub-basin receives sediment from the meltwater of perennial snowpack located in previously glaciated cirque (Arnold, 2009). The rest of the lake contains one large distal basin parallel to the lake's long axis, with Linnéelva as the dominant sediment source (Arnold, 2009). Both the eastern and western sub-basins have a maximum depth of 15 m. The deep hole in Linnévatnet is 40 meters deep and located in a distal basin (Svendsen et al. 1987). The bathymetry of Linnévatnet is shown in Figure 4.

Presently Linnévatnet is covered with ice from September to July (Snyder et al., 2000; Retelle, personal communication). Linnévatnet is protected from easterly and westerly winds by mountains but during the ice-free summer months the lake surface is susceptible to southerly winds (Boyum and Kjensmo, 1978). The watershed has a toal area of 27 km^2, 1.7 km^2 of which is glaciated (Snyder et al., 2000).

Linnédalen Bedrock Geology

The bedrock of western Linnédalen is comprised of phyllite and schist of the Precambrian Hekl Hoek Formation, and a Carboniferous carbonate-dolomite complex of the Billefjorden Group (Nelson, 2010). The bedrock of the eastern side of Linnédalen is comprised of carbonates of the Carboniferous Nordenskiödbreen formation and gypsum from the Permian Gipshuken Formation (Nelson, 2010). The Billefjorden Group is interbedded with basaltic lava flows and show evidence of an active karst system (Wei, 2010). Linnébreen and Linnéelva erode siltstones, sandstones, shale, and coal beds and transport them into Linnévatnet. Figure 5 is a bedrock map of Linnédalen.

Arctic Climate During the Holocene

The Arctic is commonly defined both as the area located north of latitude 66°N, known as the Arctic Circle, and as the area north of the 10°C July isotherm. Both are indicated in Figure 6. The arctic environment is very sensitive the effects of climate change, and therefore is a very good indicator of small and large scale changes in global climate conditions.

The Arctic climate of the Late Holocene is characterized by an overall cooling trend from 1900-100 years before present (BP), and a rapid increase in temperature in the last 100 years (D'Andrea et al., 2012). The long-term cooling trend contains two anomalous periods, the Medieval Climate Anomaly (MCA), and the Little Ice Age (LIA) indicated in Figure 7. These two periods are defined loosely in time because their effects are seen at different various intervals throughout the world and the Arctic.

The MCA is characterized as a warm period from AD 950-1250 (D'Andrea et al., 2012). During this period average global temperatures were 0.35°C warmer than the following LIA (Bradley, 2003). in Svalbard there were likely two periods of MCA warming from AD 1010-1060 and from AD 1160-1250 (D'Andrea et al., 2012). The MCA is likely the result of solar insolation, changes in North Atlantic Oscillation mode, and volcanic forcings (Bradley, 2003).

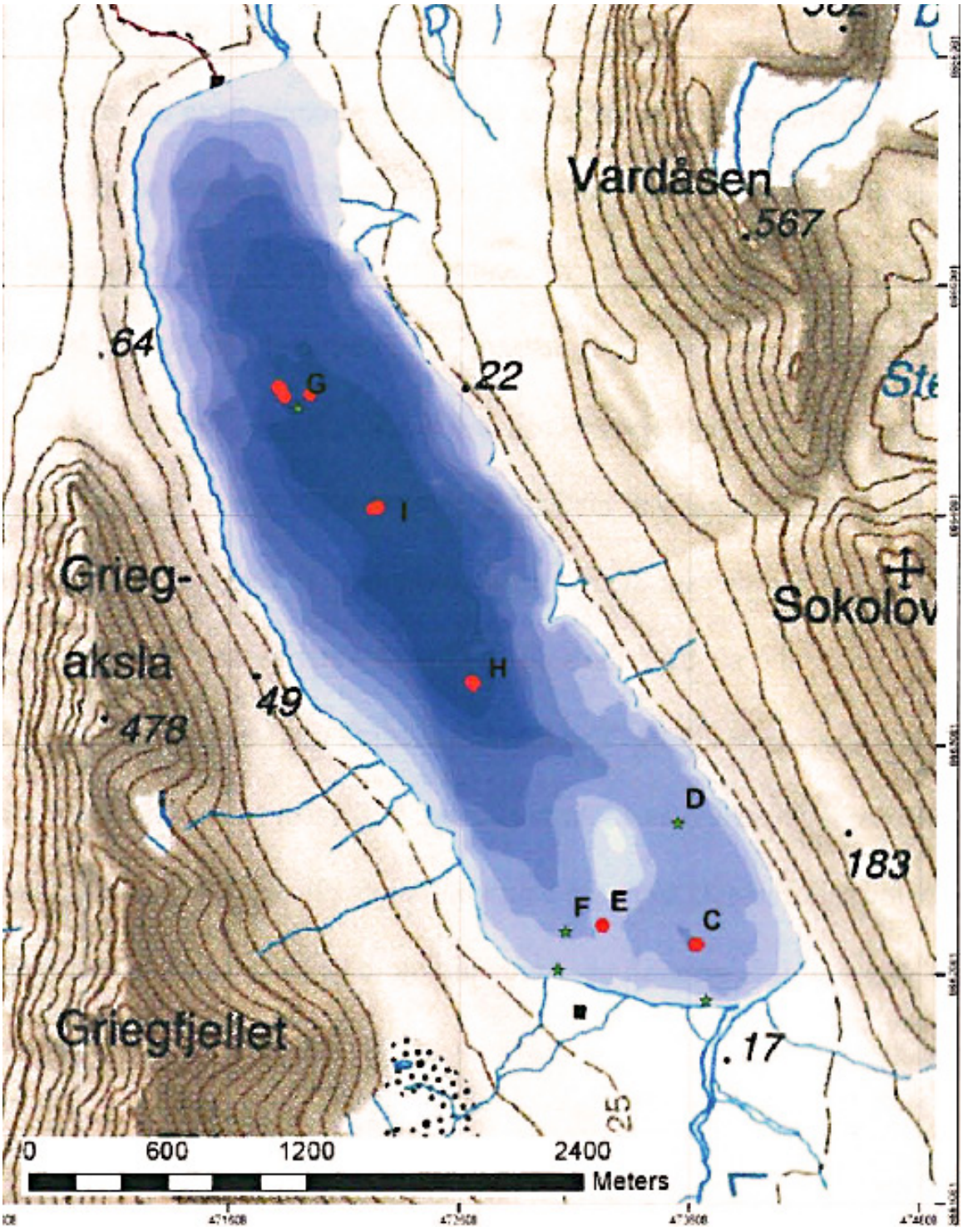

Figure 4 - A bathymetric map of Linnévatnet. Common coring sites are indicated C through I. Coring site C is located in the eastern basin and coring site F is located in the western basin. Sites H, I, and G are located in the distal basin. The cores analyzed in this study were collected from site H. (Figure from Nelson, 2010)

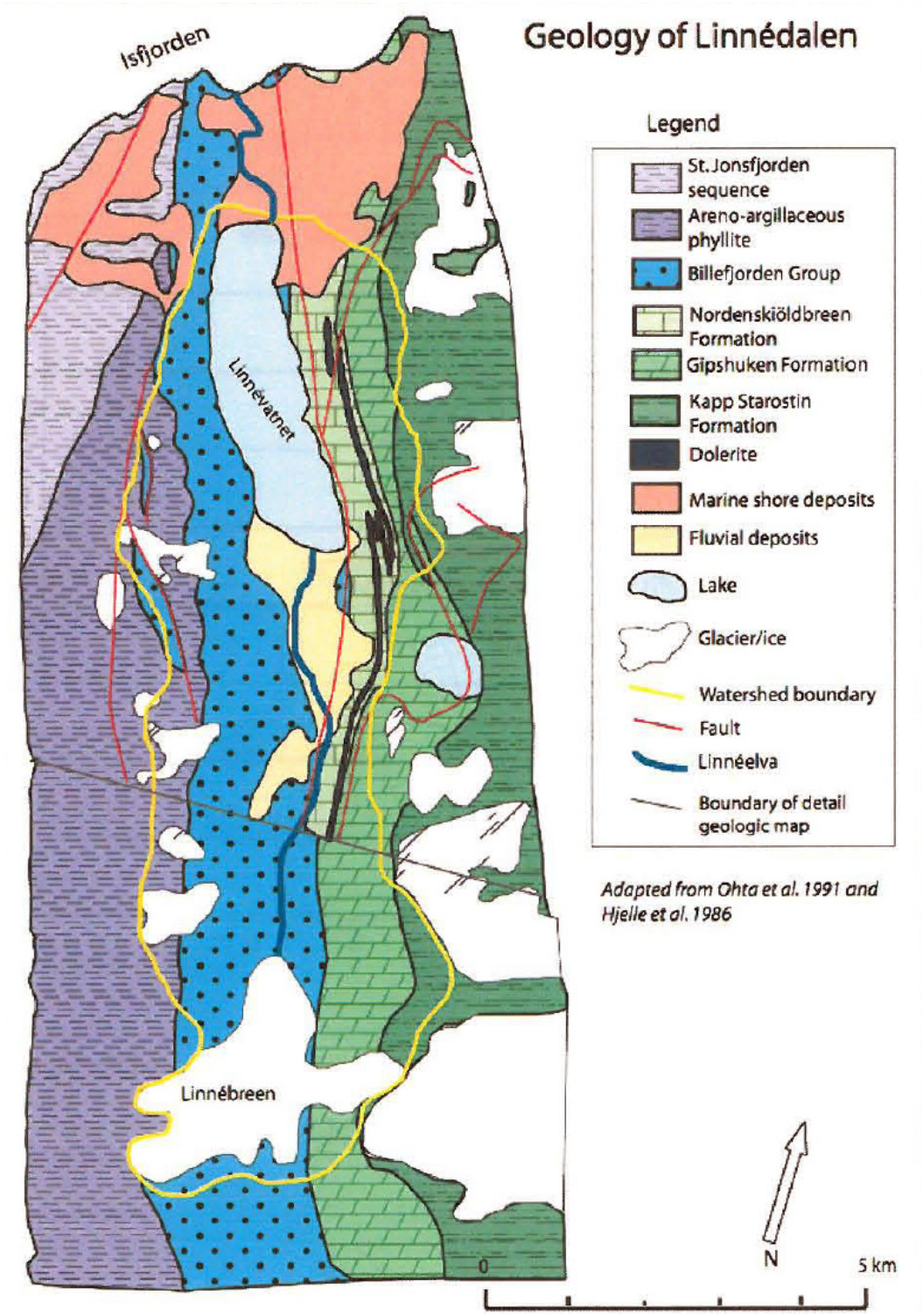

Figure 5 - A bedrock map of Linnédalen. The dominant bedrock formations are the Billefjorden Group and Gipshuken Formation. The Billefjorden Group is comprised of coal beds that have been eroded by Linnébreen and transported to Linnédalen throughout the Late Holocene (Figure from Perreault, 2009)

Figure 6 - A map showing the 1975 10°C July Isotherm in red, the Arctic Circle at 66°N in blue, and Svalbard outlined in green. (Figured modified from Nelson, 2010 from UTexas Library Map Collection)

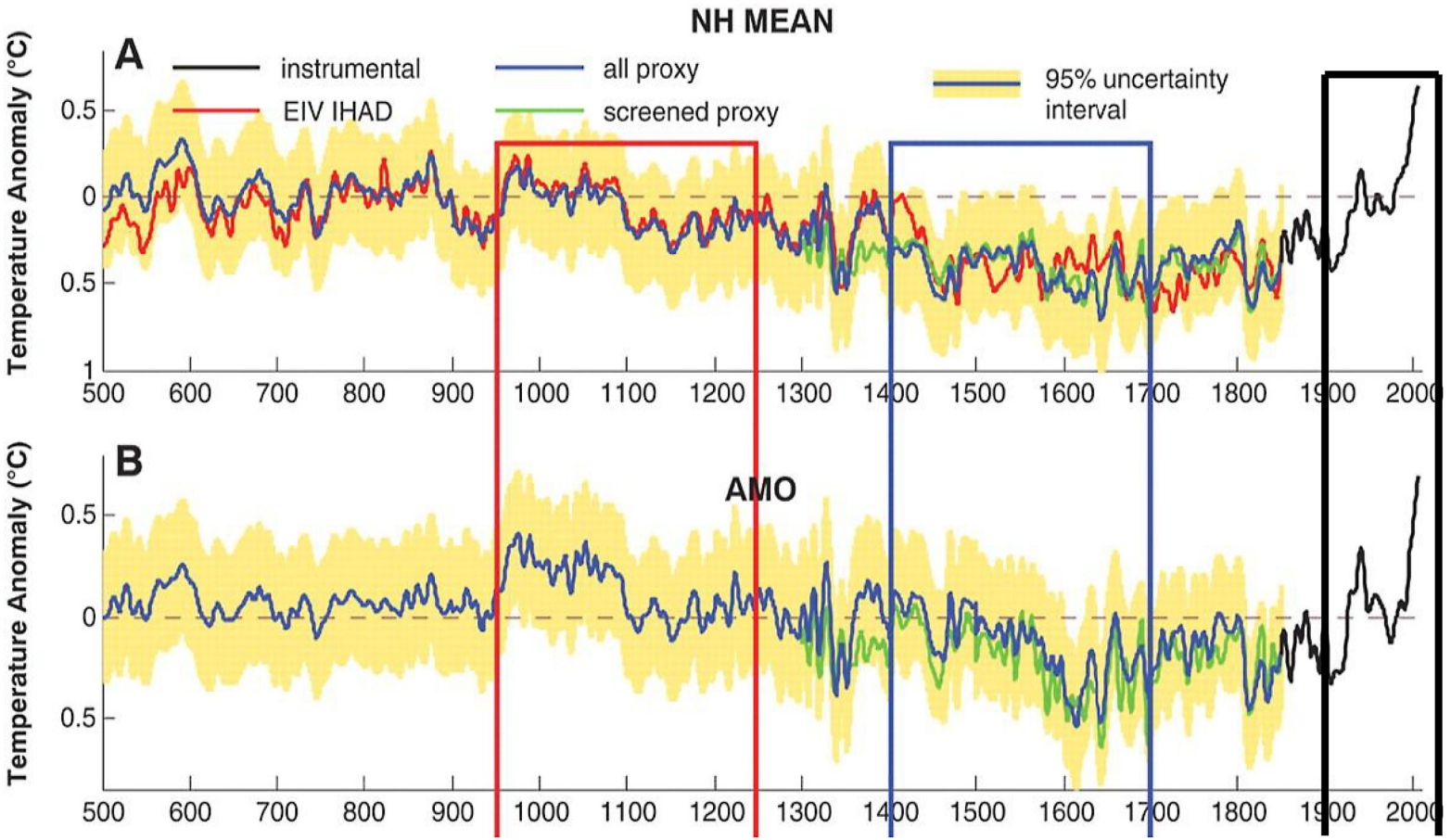

Figure 7 -Surface temperature reconstructions averaged over the Northern Hemisphere (Graph A) and the North Atlantic Multidecadal Oscillation region (Graph B). The red box indicates MWP, the blue box indicates LIA and the black box indicates 20th and 21st warming (Figure modified from Mann et al., 2009)

The LIA is a cool period that followed the MCA and lasted from approximately AD 1400-1850, although in Svalbard the effects are seen well into the 1900's as indicated by glaciers lying against their LIA moraine as late as the 1930's. The LIA is thought to be both a period of low temperatures (Humlum et al., 2005; Svendsen and Mangerud, 1997) and increased precipitation (D'Andrea et al., 2012) in the Arctic. The effects of the LIA are widespread as indicated by glacier advance throughout the northern and southern hemispheres (Denton and Karlén, 1977; Thompson, 1986). LIA cooling was most likely caused by a combination of factors including orbital, volcanic, solar forcing, and decreased northern heat transport due to reduced Gulf Stream flow (Wanner et al., 2008; Lund et al., 2006).

The current 20th-21st century warming period is clearly the most rapid change in Arctic temperatures in the last 2000 yrs. This rapid warming trend is due primarily to increased greenhouse gas concentrations (IPCC, 2007). Global temperatures are increasing at an unprecedented rate as indicated by 11 of the years between 1995 and 2006 ranking within the top 12 warmest years recorded in the instrumental record before 2006 (IPCC, 2007). In addition, average temperatures in Svalbard from 1987-2009 are 2-2.5 °C warmer than the temperatures experienced during the MCA (D'Andrea et al., 2012). The present warming is predicted to continue as atmospheric CO_2 concentrations increase and warming is amplified by ice and snow albedo feedbacks. The greatest shifts in temperatures are expected to occur in the Arctic (Kattsov et al., 2005).

Glacial and Climatic History of Svalbard

During the last glacial cycle, 115,000-10,000 BP, Svalbard was likely subject to three major glaciations (Ingolfsson, 2006). During these glaciations the Barents Sea Ice Sheet covered all of Svalbard (Ingolfsson, 2006). The last glacial maximum (LGM) ended rapidly approximately 14,000-10,000 BP. This was followed by sea level rise of approximately 70-80m (Ingolfsson, 2006; Mangerud and Svendsen, 1990). Evidence from Linnévatnet (coastal Isfjorden) and Billefjorden (interior Isfjorden) both indicate little to no glacial activity on Svalbard between LGM through the Holocene Hypsithermal Interval until approximately 4,500 yrs BP (Svendsen and Mangerud, 1997). Glacier growth began again on Svalbard approximately 4,500 yrs BP and peaked first at 2,500 yrs BP and then subsequently reached their Holocene maximum during LIA (Svendsen and Mangerud, 1997). Since the end of LIA in the early 1900's, Svalbard glaciers have retreated and their margins are located behind their LIA moraines (Ingolfsson, 2006).

Linnédalen Deglaciation

Late Weischelian glaciation on Kapp Linné lasted from approximately 17,500 BP to 12,500 BP (Mangerud and Svendsen, 1990). Following the deglaciation sea level was approximately 70 m higher than the present and Linnédalen was a fjord (Svendsen and Mangerud, 1997). This is indicated by marine terraces as high as 87 m above sea level in Linnédalen (Mangerud and Svendsen, 1990) and by marine sediment in Linnévatnet the oldest of which was deposited after 12,500 BP (Svendsen and Mangerud, 1997). Linnévatnet was isolated from the sea at 9,600 BP as indicated by

the transition of marine sediment to lacustrine sediment in Linnévatnet (Svendsen and Mangerud, 1997). The lack of laminations and coal content in the sediment record of Linnévatnet suggest there was no glacial activity within the Linnévatnet catchment area from 9,600 BP to 4,400 BP (Svendsen and Mangerud, 1997). Increases in total organic carbon (TOC) values and annual laminations at 4,400 BP indicate the formation of glaciers within the catchment area, specifically the formation of Linnébreen (Svendsen and Mangerud, 1997). Glacial maxima at 2,800 BP, 2,400 BP, 1,500 BP and LIA glacier growth are indicated by spikes in TOC in the Linnévatnet sediment record (Svendsen and Mangerud, 1997). Since the period of no glacial activity in Linnédalen, from 9,600BP to 4,400BP, there have been two periods of significant glacial growth from 4,400-4,000BP and the last 800 years (Svendsen and Mangerud, 1997).

Present climate of Svalbard

The present climate on Svalbard is characterized as High Arctic polar desert. It receives <190 mm of annual precipitation, less than half the precipitation of other Arctic regions and less than one quarter than that of the subarctic (French and Slaymaker, 1997). At sea level, average temperatures are -6°C. Temperature measurements from locations on Spitsbergen show an overall warming trend over the last 100 years (Nordli and Kohler, 2004).

The climate of Svalbard is heavily influenced by both patterns of atmospheric and ocean circulation and is located along many major conduits of heat transfer into the Arctic (D'Andrea et al., 2012). Svalbard is currently located on the boundary between cold polar air and warmer air from the North Atlantic (Ingolfsson, 2006). This boundary is the primary atmospheric moisture pathway from the Atlantic to the Arctic (D' Andrea et al., 2012). Precipitation in Svalbard is closely linked to North Atlantic Oscillation with positive NAO values resulting in increased precipitation (D'Andrea et al., 2012.) In addition, a northern extension of the Gulf Stream, the Western Spitsbergen Current (WSC) flows northwards bringing warm water along the western coast of Spitsbergen. The WSC has a major influence on all of Svalbard but specifically affects the local climate of Isfjorden and may be responsible for differences in climate conditions experienced by Kapp Linné and arctic-wide climate conditions (Rassmussen et al., 2012; D'Andrea et al., 2012).

Linnévatnet Sediment Record

The Linnévatnet sediment record consists of 6 meters of marine sediment, followed by 6 meters of lake sediment (Svendsen et al., 1987). The bottom of the lake sediment interval contains a section of black monosulphide stained laminations reflecting anoxic conditions following the separation of Linnévatnet from the sea approximately 9,600 BP (Svendsen et al., 1987). The overlying lacustrine sediment interval is primarily massive with some silt laminae and low TOC content. The lack of laminations and TOC suggest that glaciers were not prevalent within the watershed (Svendsen and Mangerud, 1997). As glacial activity increased slowly, beginning approximately 7,500 years ago, the massive lacustrine sediments transitioned into an interval of diffuse laminations (Svendsen and Mangerud, 1997). Then as glaciers, specifically Linnébreen, became well established in Linnédalen

around 4,400 yrs BP the sediments deposited in Linnévatnet became strongly laminated (Svendsen and Mangerud, 1997). This gradual shift is also reflected in TOC measurements from this section of the sediment record (Svendsen and Mangerud, 1997). The remainder of the sediment core extending to the present consists of well-defined laminations of clay, silt and sand. The changes in the lithostratigraphy of the Linnévatnet sediment record as analyzed by Svendsen and Mangerud (1997) is shown in Figure 8. The presence of laminations in the sediment record indicates a lack of benthic biota in Linnévatnet which ensures the sediment record is preserved as it deposited (Nelson, 2010)

Sediment Distribution

The distribution of sediment in Linnévatnet is a function of sediment source, the rate of sediment supply, particle size, winds, waves and the Coriolis Effect. At the southern end of Linnévatnet the proximal eastern sub-basin receives sediment from Linnéelva while the proximal western sub-basin receives sediment from the meltwater channel of a previously glaciated cirque which now sustains perennial snowpack (Arnold, 2009).The distal basin reflects only sediment inputs from Linnéelva because Linnéelva provides a higher volume of sediment at a higher rate than any other inflow the sediment in this deep basin (Nelson, 2010). In the two proximal basins sedimentation rates are 1.5 mm/yr and there is a strong correlation between grain size, stream discharge, and storm events (McKay, 2005). In the distal basin sedimentation rates are approximately 0.15 mm/yr and grain size has a lower correlation to weather events (McKay, 2005; Nelson, 2010).

The Linnévatnet primary sediment source is located at the southern end of the lake. This results in sedimentation rates that decrease to the north and the thickness of lacustrine sediments in the distal basin decreases towards the north end of the lake as shown in Figure 9 (Nelson, 2010; Svendsen et al., 1987). The decrease in particle size to the north within Linnévatnet is also shown in Figure 9 (Nelson, 2010).

This sediment distribution is due to the fact that large particles settle faster than fine grained particles. This results in a decrease in lamination thickness from proximal to distal locations. Therefore, a sediment core from a distal location will contain a longer temporal record than a core of the same length from a proximal location. However, as described above, distal locations are less sensitive to intra-annual events and may only contain records of large stochastic sediment flows related to earthquake triggered slumping events. Since this study is focusing on yearly, decadal, and century-scale change a distal coring location was chosen.

The Coriolis Effect is the deflection of moving objects within a rotating reference frame. In the northern hemisphere, the earth's rotation is counter clockwise and moving objects are deflected to the right. This effects sediment distribution in Linnévatnet by deflecting sediment moving through the lake to the right. The resulting grain size distribution ranges from coarse to fine both from proximal to distal and from right to left. The distribution of sediment can be additionally altered by wind and waves. A simplified version of the resultant cumulative effect and sediment distribution in Linnévatnet is pictured in Figure 10.

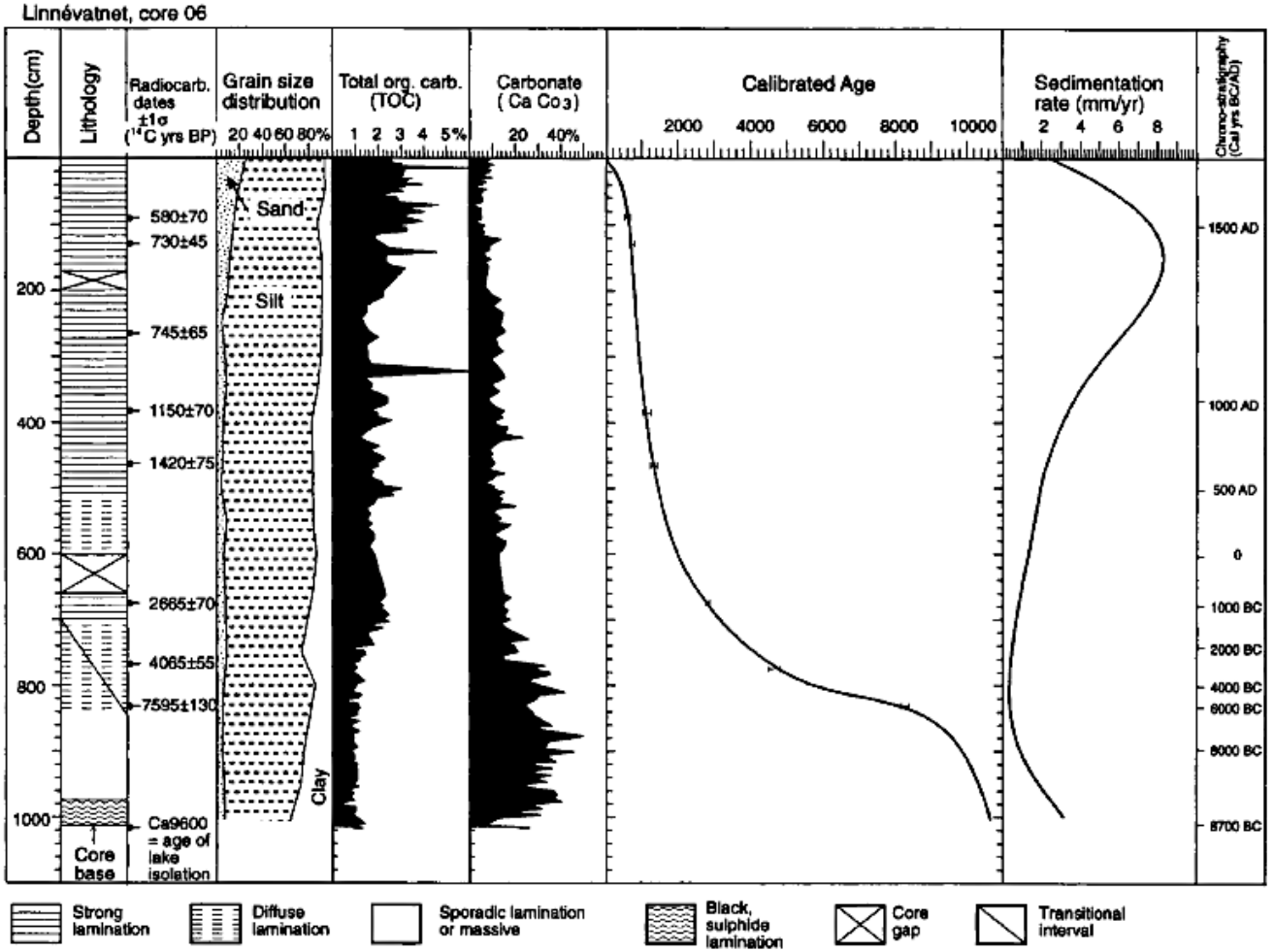

Figure 8 -A lithostratigraphic column from a Linnévatnet sediment core collected and analyzed by Svendsen and Mangerud (1997). The periods of glacier activity in Linnédalen are indicated by spikes in TOC. (Figure modified from Svendsen and Mangerud, 1997)

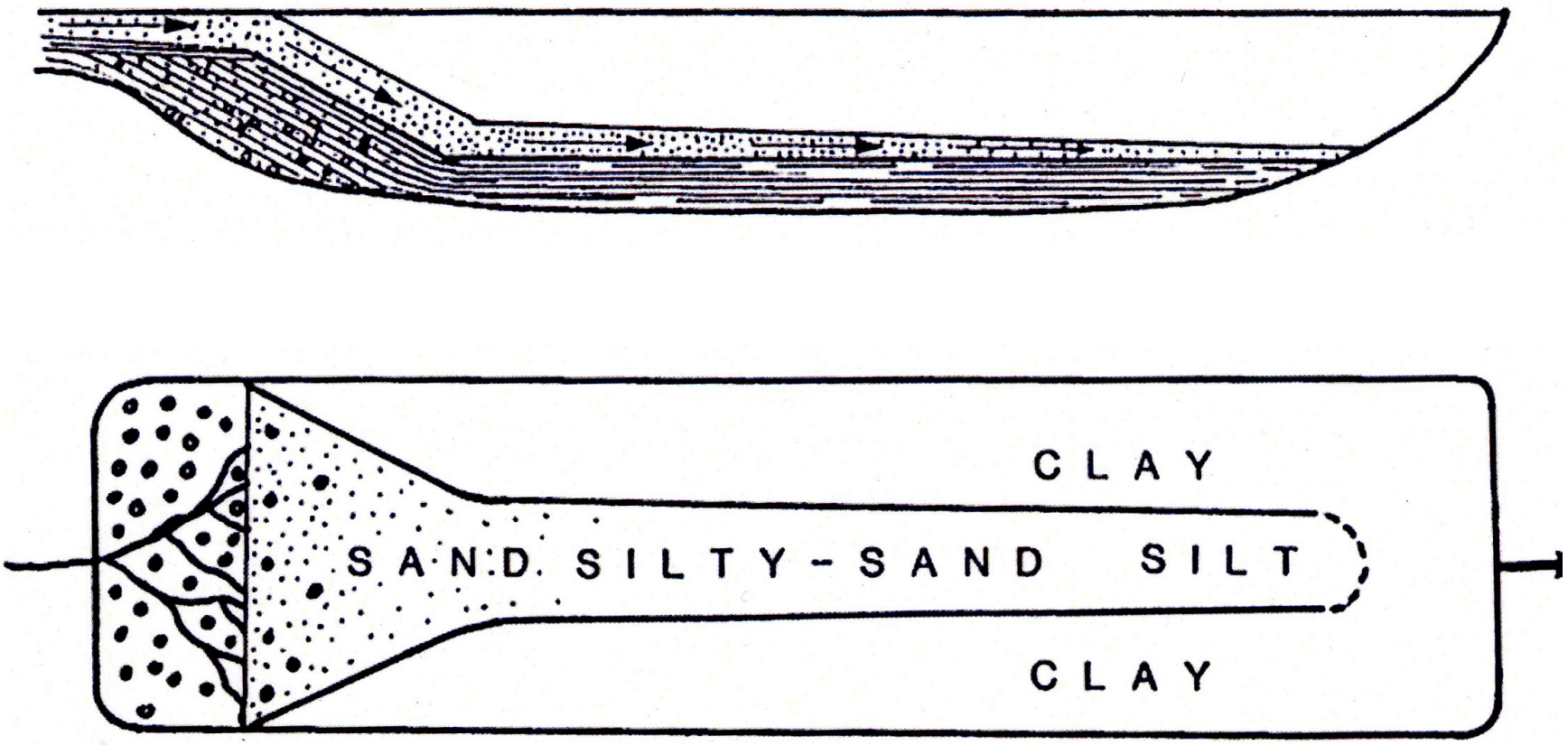

Figure 9 - A schematic diagram illustrating the distribution of sediment in Linnévatnet. Diagram A shows the thinning of lacustrine sediment as distance from the source increases. Diagram D shows the showing the decrease in particle size of lacustrine sediments as distance from the source increases (Figure modified from Smith and Ashley, 1985)

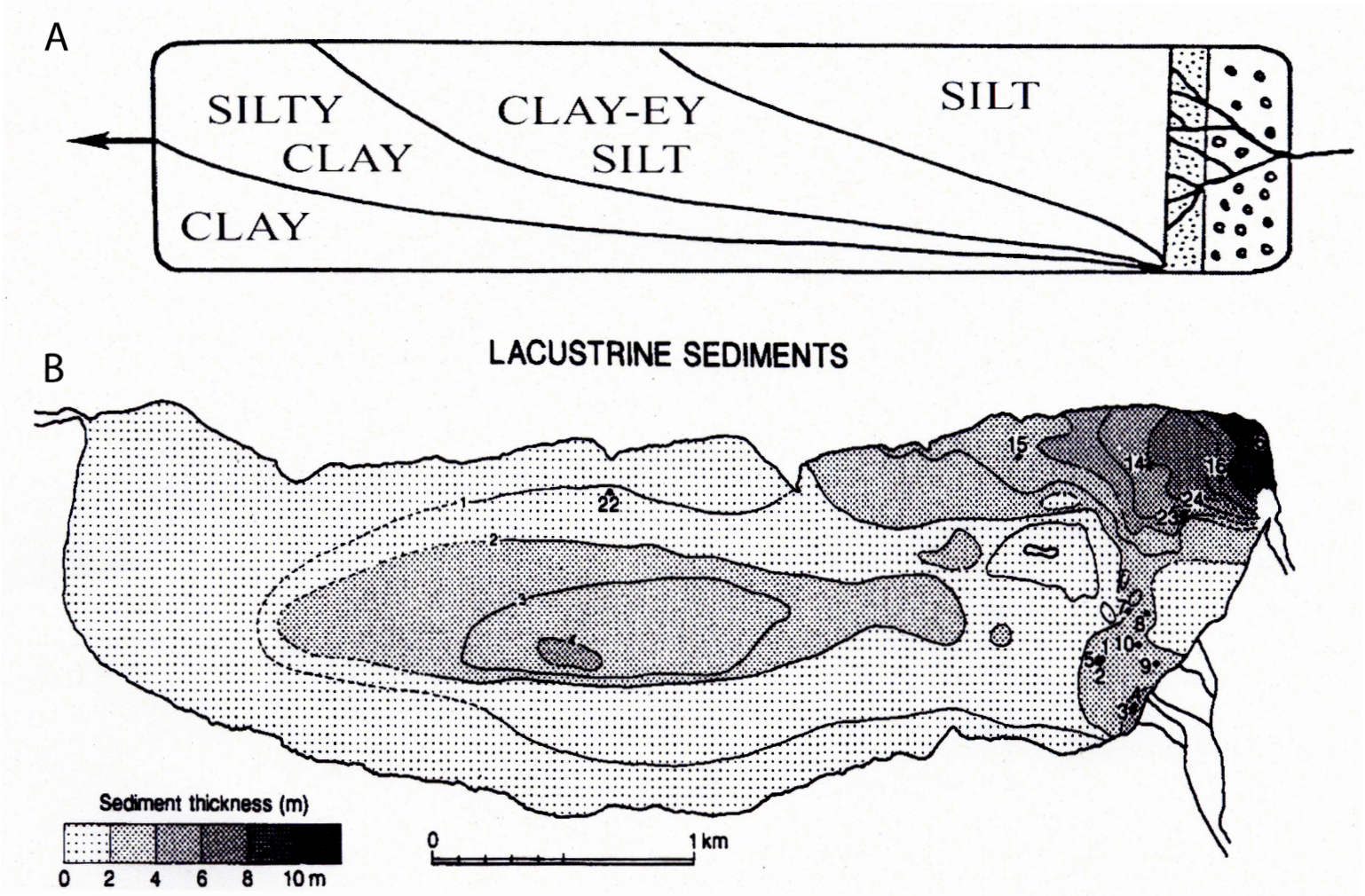

Figure 10- The upper diagram (A) is a schematic of lacustrine grain size distribution as a result of the Coriolis Effect. The lower diagram (B) is a bathymetric map of Linnévatnet with sediment thickness shown. It is clear that the distribution of sediment and distribution of particle size in Linnévatnet is a function of sediment source, rate of sediment supply, particle size, winds, waves and the Coriolis Effect. (Part A - modified by Arnold, 2009 from Smith and Ashley, 1985; B- modified by Arnold, 2009 from Svendsen et al., 1989.)

Implications of the Varved Sediment Record

Linnévatnet accumulates varved deposits which consist of summer-winter couplets of coarse and fined grained laminations. Time lapse cameras from ongoing research by the Svalbard REU indicate spring snow melt occurs rapidly, primarily within a two week period in mid-July (Nelson, 2010). During this melt period flow from Linnéelva is high and transported sediment has relatively coarse grain size (Nelson, 2010). Overall, sediment input gradually decreases through the summer from this initial melt period until it approaches zero in mid-September (Nelson, 2010). During this periods spikes in Linnéelva discharge and sediment flow into Linnévatnet result from precipitation events and periods of high melting. In mid-September sediment input stops when Linnévatnet and Linnéelva freeze over (Nelson, 2010). From October to June Linnévatnet is ice covered, allowing fine grained particles to settle out of suspension. The resulting annual couplet is comprised of a tan colored coarse grained layer overlain by a dark grey fine grained layer (Nelson, 2010). The annual periodicity of these laminations has been confirmed by sediment trap analysis by the Svalbard REU, and plutonium age dating (Nelson, 2010). This allows for varve couplets to be counted along the core, and high resolution depth vs. time relationship can be established at many of the coring sites.

The physical characteristics of the varves in the Linnévatnet sediment record can be measured and interpreted to accurately determine glacier mass balance, and weather conditions such as in Linnédalen (Svendsen and Mangerud, 1997; Leemann & Niessen, 1994). This interpretation, however, is complex and requires the factoring in of many variables. Both the advancement and retreat of Linnébreen and other cirque glaciers can result in the increase of glacially derived sediments (Svendsen and Mangerud, 1997). When the glaciers advance the area affected by erosion increases, and the sediment sources moves closer to the lake (Svendesen and Mangerud, 1997). When the glaciers retreat more meltwater is released and glacial sediments are reworked by the meltwater stream (Svendsen and Mangerud, 1997). Due to the complexity of these processes previous studies on how weather conditions relate to the deposition of lacustrine sediments in Linnévatnet by Svendsen and Mangerud (1997), Arnold (2009), Nelson (2010), and Wei (2010) are used to correlate the physical characteristics of the sediment to potential paleoenvironmental conditions.

Summary of Goals

This study aims to reconstruct Late Holocene paleoclimate conditions in Linnédalen located in coastal western Spitsbergen, from the varved sediment record of proglacial lake Linnévatnet. It is known from previous studies that the sediment record is closely tied to glacial activity in Linnédalen, and specifically in the last 4,400 yrs to the growth and retreat of Linnébreen (Svendsen and Mangerud, 1997). Using this sediment-glacier relation and the sensitivity of glaciers to shifts in climate conditions the sediment record can be used to reconstruct conditions through time. The first step in this reconstruction is to decipher the climate signal from the sediment record. The second step is to interpret the climate signal with respect to other relevant paleoclimate reconstructions and develop a picture of climate conditions in Linnédalen during the Late Holocene.

This study will analyze both a long and short core from a distal site in Linnévatnet. The distal location will dampen the effects of short-term storm events and will primarily record the effects of yearly and decadal climate change on the glacier, meltwater stream, and lake system in Linnédalen. The paleoclimate reconstruction presented in this study will be based upon the short core as it has been studied in more depth. Future work on the long core will allow for extension of this paleoclimate reconstruction further back into the Holocene.

Methods

The sediment record of the proglacial lake Linnévatnet was chosen for paleoclimate analysis and reconstruction because it documents changes in glacier mass balance and climatic conditions in Linnédalen (Svendsen and Mangerud, 1997). These changes are best recorded through variations in the physical character of the sediment (Svendsen and Mangerud, 1997; Leemann & Niessen, 1994). Therefore, the methods used in this study focused on obtaining a continuous undisturbed sediment record, analyzing how its physical characteristics vary with depth, and developing an accurate age model.

From the large amount of limnologic research and coring that has been performed at Linnévatnet it was determined that the best coring location for paleoclimate reconstruction is Site H, shown in Figure 4 (Wei, 2010). Site H is located at the proximal end of the large distal basin. This location is less sensitive to intra-annual sediment pulses than a proximal location and has a higher sedimentation rate than more distal locations (Wei, 2010). The sedimentation rate at this location allows for the formation of annual laminations that are thick enough for thorough analysis but also thin enough that sediment cores contain a long record.

Field Methods

Sediment cores were collected from Linnévatnet at site H in May, 2012 through holes drilled in the ice. Short cores were collected with a K-B universal corer. This coring device collects cores in clear plastic tubing with an interior diameter of 6.6 cm and utilizes a one-way valve to ensure sediment is not disturbed or lost as it is pulled up through the water column. Four cores were collected with the K-B universal corer. LH-1 was collected May 7th and cores LH-2, LH-3, and LH-4 were collected May 9th. LH-4 is the longest of these cores at 49.5 cm in length and was analyzed in this study. A long core was also collected from the same site on May 7th with a modified Nesje percussion coring device. The core, LH-Long, is 1.4 meters in length and is partially analyzed in this study. The percussion coring device relies on a piston to collect sediment cores in aluminum tubing and as a result the top few centimeters of a long core can be disturbed. After the cores were collected they were allowed to dewater for over a month and were then packed for shipment to Bates College in Lewiston, Maine for analysis.

Lab Methods

Cores LH-4 and LH-Long were processed in the Bates College Sedimentology Lab. First, each core was split into a working and an archive half. The plastic core casing on the short cores was cut with a table saw and a dremel tool. The aluminum casing on the long core was cut with power cutting shears. Once the core casing was split the cores were cut in half lengthwise with fishing line. A bead of deionized water was placed along the cut made by the fishing line and the two halves of the sediment core were separated. Both cores were wrapped in plastic and stored horizontally in a fridge

when not being analyzed. The working half of the core was used for subsampling-based analyses while the archive half was used for non-destructive analyses.

Subsampling Analysis

The subsampling analyses performed on the cores included bulk density, dry density, percent loss on ignition (% LOI), and grain size. All of these analyses were performed on core LH-4, while only grain size analysis was performed on core LH-Long. In addition, core LH-4 was also subsampled for Plutonium age determination, and both cores were subsampled for thin section creation and Geotek Multi-Sensor Core Scanner analysis.

Bulk density, dry density, and %LOI, were measured from a 1 cm^3 cube of sediment sampled every centimeter along the length core LH-4. In order to obtain a 1 cm^3 cube of sediment an open ended aluminum cube with interior dimensions of 1 cm x 1 cm x 1 cm was pressed into the sediment. Once the top edge of the cube was flush with the top of the sediment a tool was used to separate the bottom of the cube from the core. Then the aluminum cube, now full of sediment, was lifted free from the core. Each 1 cm^3 cube was massed to determine the bulk density (g/cm^3). The 1 cm^3 cube of sediment was then dried in an oven at 100°C for 12 hours. The dried sediment was then massed to determine the dry density (g/cm^3). % Water was calculated from these two values.

The 1 cm^3 sediment cubes were then placed in a furnace at 550°C for an hour to roast off all organic material. The cube of sediment was massed one final time to obtain roasted density (g/cm^3). % LOI was calculated % LOI values can be affected by both the organic content of the sediment record and water included in clay minerals that is not lost during the drying phase.

Grain Size analysis was performed on both cores (LH-4 and LH-Long) with a Beckman Coulter LS 13 320 Particle Size Analyzer (PSA). The PSA measures particle size through single wavelength laser analysis. A laser is shown through the prepared sample solution and from the resulting pattern grain size can be determined. For this analysis a 0.125 cm^3 volume (1 cm depth x 0.5 cm width x 0.25 cm length along core) of sediment was sampled centered at 1 cm intervals along core LH-4 and centered at 2 cm intervals along core LH-Long. The volume of sediment was chosen because it resulted in obscurity values within the optimal range (10-20%) for a series of test samples. Each subsample was placed in a 47 mL Oak Ridge centrifuge tube. 1 mL of hydrogen peroxide was added immediately after subsampling to disintegrate the organic matter within the sample. 12-24 hours later 20 mL of deionized water and 17 mL of dispersant (0.7 g/L sodium metaphosphate) were added to each sample. The samples were then shaken for 1 minute and sonicated with a sonic dismembrator for 1 minute to deflocculate clumps of fine particles. Each sample was run three times on the Beckman Coulter PSA and the mean, median, and 90^{th} percentile of each run was recorded. For all but three depths the reported mean and median grain size were the average of the three runs. The final run from samples collected from 2 cm, 4 cm and 6 cm depth in core LH-Long were discarded because they resulted in anomalous bimodal distribution and very high 90^{th} percentile values. It is likely that the skewed values are the result of air bubbles within the instrument. For these three samples the data presented is the mean and median grain size averaged from the first two runs.

Thin Section Creation

Thin sections were created by subsampling the entire length of both cores. The subsamples for each thin section overlapped by 1 cm to ensure complete core stratigraphy was included in at least one thin section. Each subsampling box was formed from newspaper offset printing plates and was 1 cm deep x 2 cm wide x 7cm in length along core. Holes were drilled in each sampling box with a 1/24th inch drill bit spaced approximately 2-3 millimeters apart to allow for acetone and epoxy to penetrate the box later in the procedure. The subsampling boxes were pressed completely into the sediment in an alternating left-right pattern along the core. To remove the subsampling box fishing wire and/or a U-shaped cutting tool were passed underneath the box. The filled box was then removed with a metal spatula. Any excess sediment was removed by cutting a fresh face on the open side with fishing line and wiping the sides with Kim-wipes. The boxes were then placed parallel to each other in a flat-bottomed plastic container. The upper 7 centimeters of core LH-4 was subsampled 3 times to ensure the upper part of the core would be well preserved during thin section creation. The remainder of the core was subsampled as described above with 1 cm of overlap. This resulted in 10 thin sections for core LH-4 labeled 1a, 1b, 1c and 2-8 each 7 centimeters in length. Core LH-Long was subsampled as described above and thin sections were labeled 9-30.

All subsamples were dehydrated through a series of acetone exchanges, a procedure modified from Nelson (2010). The sediment samples were submerged in acetone for 8 hours and covered with a lid. Acetone was carefully poured into the corner of the container to minimize any disturbance of the sediment. After 8 hours the acetone was removed with a volumetric pipette and its specific gravity was measured. If the measured specific gravity did not match the specific gravity of pure acetone then the samples were submerged with fresh acetone for 8 more hours. This process was repeated with Histological Grade acetone until the specific gravity of the acetone approached 0.792. After this point the samples were submerged in EM Grade acetone for any additional exchanges. Once the specific gravity of the EM Grade acetone used for soaking remained at 0.791 for two exchanges it was assumed that all water had been removed. The acetone specific gravity measurements for core LH-4 is shown in Figure 11.

The sediment samples were then impregnated with an epoxy-resin mixture through a series of four acetone/epoxy exchanges. The epoxy-resin mixture was comprised of cyclohexyl carboxylate (ERL 4221), diglycidol ether of polypropyleneglycol (DER), nonenyl succinic anhydride (NSA), and dimethylaminoethanol (DMAE). These four reagents were measured gravimetrically immediately before use with a mass ratio of ERL:DER:NSA:DMAE of 106.7:37.1:153.5:2.6. The acetone/epoxy baths contained EM grade acetone and epoxy in a volumetric ratio of 50/50, 25/75, 0/100 and 0/100. Each exchange lasted 10-14 hours, and containers were covered with lids. After the samples were submerged for the final time in 100% epoxy, the containers were left uncovered in a fume hood. After 12 hours the samples were placed in a 50°C oven for 72 hours until the hardened epoxy couldn't be scratched or depressed by a fingernail. The blocks of hardened epoxy, Figure 12, were then popped out of their containers, and trimmed with a band saw. The sediment slabs were sent to Quality Thin Sections in Tucson, Arizona to be cut, polished, and mounted on slides. The final LH-4 thin sections

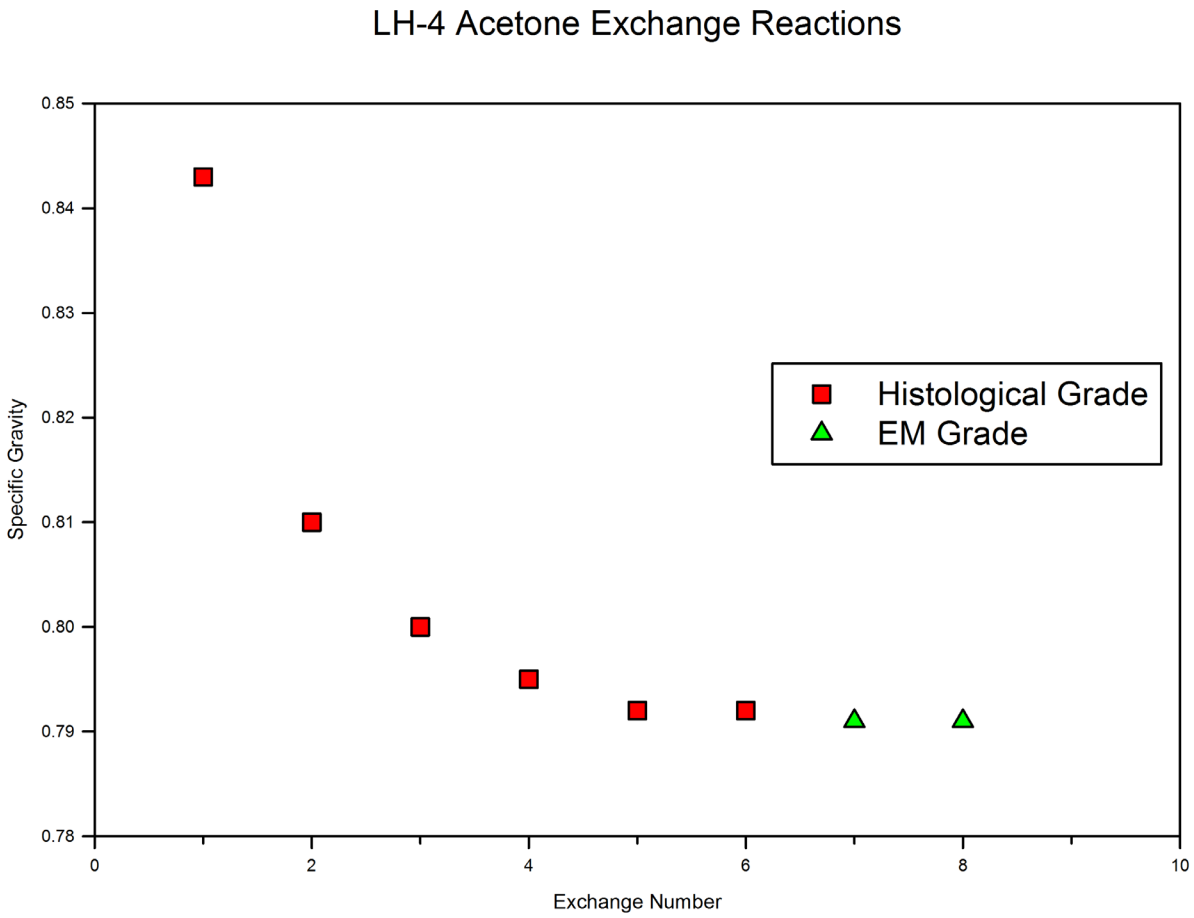

Figure 11 -A plot of specific gravity measured after each acetone exchange during LH-4 thin section creation. The curve for LH-Long is ver similar. The red squares represent Histological Grade acetone, which was used until specific gravity approached 0.791. The green triangles represent EM Grade acetone which was used for the final two exchanges.

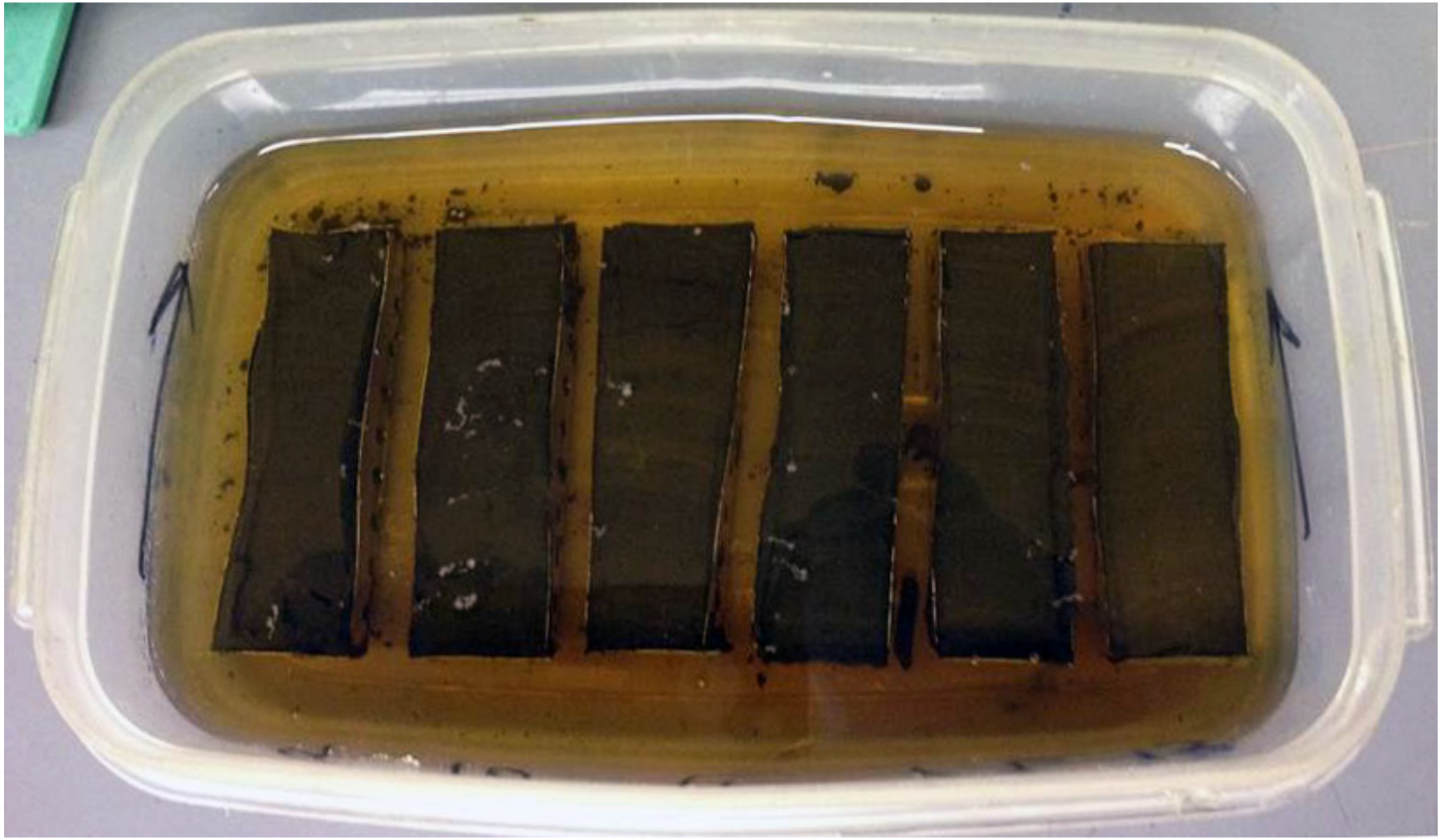

Figure 12 -A photograph of six LH-4 subsamples submerged in their final bath of 100% epoxy. The arrows indicate the upwards direction. The hardened block of thin sections was trimmed with a bandsaw and then sent away to be ground and mounted on slides. All thin sections created overlapped by 1 cm to ensure complete core stratigraphy was included in atleast one thin section.

contained the upper 48 cm of the core and were analyzed in this study. The LH-Long thin sections were made and will be analyzed in a future study extending the paleoclimate picture developed from the analysis of core LH-4.

Plutonium Age Determination

Subsamples were collected from core LH-4 for plutonium dating as defined by Ketterer et al. (2004). Sampling was performed from the top of the core to a depth of 10 cm. 20 subsamples 0.5cm in length along core were collected in continuous column down the core. Based on calculations and varve counts performed by Wei (2010) from Site H cores it was determined that sediment from a depth of 10 cm related roughly to the early 1900's. This allowed for sufficient baseline plutonium levels to be collected before the spike in plutonium that is expected 1952 and the maximum at 1963. The annual periodicity of the lamination couplets was confirmed by comparing this independent dating method with lamination couplet counts and thickness measurements.

Lamination Counts and Thickness

The completed thin sections were analyzed with a flatbed scanner. This allowed for a typical lamination sequence within the sediment record to be well-defined visually and for varves to be counted and their thickness measured. The thin sections were scanned with an Epson V750 Pro Scanner at 3200 dpi in both transmission (lit from behind) and reflective modes (lit from front). The scanned image was optimized by adjusting the pre-scan (preview) histogram so the scanned image would best record color and luminance information from the sediment within the thin section. In Adobe Photoshop both the scans were adjusted with a brightness/contrast adjustment layer and an unsharp mask was applied (typical parameters for unsharp mask were Amount = 80%, Radius = 9.4 pixels, Threshold = 7 levels). After both scans were optimized, the scan with the clearest lamination sequences and winter-summer contacts was chosen. The core was then reconstructed in Photoshop using marker beds and the 1 cm of overlap to correctly align the thin section scans. Note that marker beds proved more helpful aligning the scans due to the varying amounts of sediment lost from the top and bottom of the section when they were ground and mounted on slides.

The lamination couplets were then counted and measured from the reconstructed core using tools in Photoshop. Graded beds identified as turbidites were not included in this analysis but were counted and measured separately. The first step in thin-section analysis was to place three vertical guidelines on top of each thin section scan. For each guideline along each thin section horizontal lines were drawn with the "Single Row Marquee Tool" where the vertical guideline crossed the contact between the top of a dark winter layer and bottom of light colored summer layer. For each thin section the number of varves counted from the three guidelines varied by ± 4%.

The whole-core varve count was made primarily by counting horizontal lines drawn along the center-most guidelines, where lamination deformation was minimal. However, the other horizontal lines drawn were helpful in interpreting sections where varves were not well defined across the entire thin section due to thinning of the sediment at the thin section edge. Care was taken to ensure that

varves contained in multiple thin sections were only counted once. The uncertainty of varve counts was determined by the method suggested by Ojala et al. (2012) and was based on the variation of three counting cycles performed on all LH-4 thin sections. In most cases counting variations were the result of interpreting thin couplets within a larger couplet as either annual or sub-annual.

Varve thickness was measured from the horizontal lines that were used in the whole core varve count. The Photoshop layers that contained the horizontal lines were copied and edited to create a new layer that included only one line marking the upper most limit of each winter layer. The area between each consecutive pair of horizontal lines was selected with the "Magic Wand Tool" by clicking in the blank area between the lines. The dimension of this area in pixels was then recorded using the "Measurement Log" window. This data was then exported as a tab-delimited text file and opened in Microsoft Excel. 1 pixel was added to each value in the height column to account for the 1 pixel taken up by the thickness of each horizontal line. The height of each selected area (varve thickness) was converted to millimeters using the 3200 dpi value of the scanned images. This value defines that each inch is represented by 3200 pixels in the scanned image. This relationship was confirmed by scanning a metric ruler and performing the same measurement on the ruler scan. Using the dpi conversion factor varve thickness values were converted from pixels to inches to millimeters. The uncertainty associated with varve thickness measurements was determined by measuring varve thickness three times on a series of diffuse varves and calculating the variation in thickness measurements.

Nondestructive Analysis

A stratigraphic log was created from the archive half of each core. The log recorded qualitative sedimentary characteristics along the core such as color, texture, grain size, and visual changes in lamination thickness. The physical characteristics and depth of marker beds to be used in the correlation of core LH-4 and LH-Long were also recorded. Quantitative nondestructive analyses were performed at the UMASS Geosciences Hartshorn Quaternary Lab. The archive half of each core was subsampled with a 1-inch wide U-channel and was then processed for magnetic susceptibility, color spectra, and imaging with a Geotek multi-sensor core scanner. The Geotek scanning device, shown in Figure 13, recorded continuous high resolution line-scan imagery of the subsampled U-channel and also recorded magnetic susceptibility and color spectra measurements at 0.5 cm intervals. Magnetic susceptibility readings were used in conjunction with the marker beds recorded in the stratigraphic log to correlate core LH-4 and LH-Long.

Comparison with Climate Records and Reconstructions

To determine the validity of the physical characteristics of the Linnévatnet as paleoclimate proxies they were compared to climate records and reconstructions from Svalbard. The physical characteristics of the sediment record were compared to the longest available instrumental record in Svalbard from the weather station located at Green Harbour/Svalbard airport since 1911 (Nordli and Kohler, 2004) and to two climate reconstructions in Svalbard. The two reconstructions were

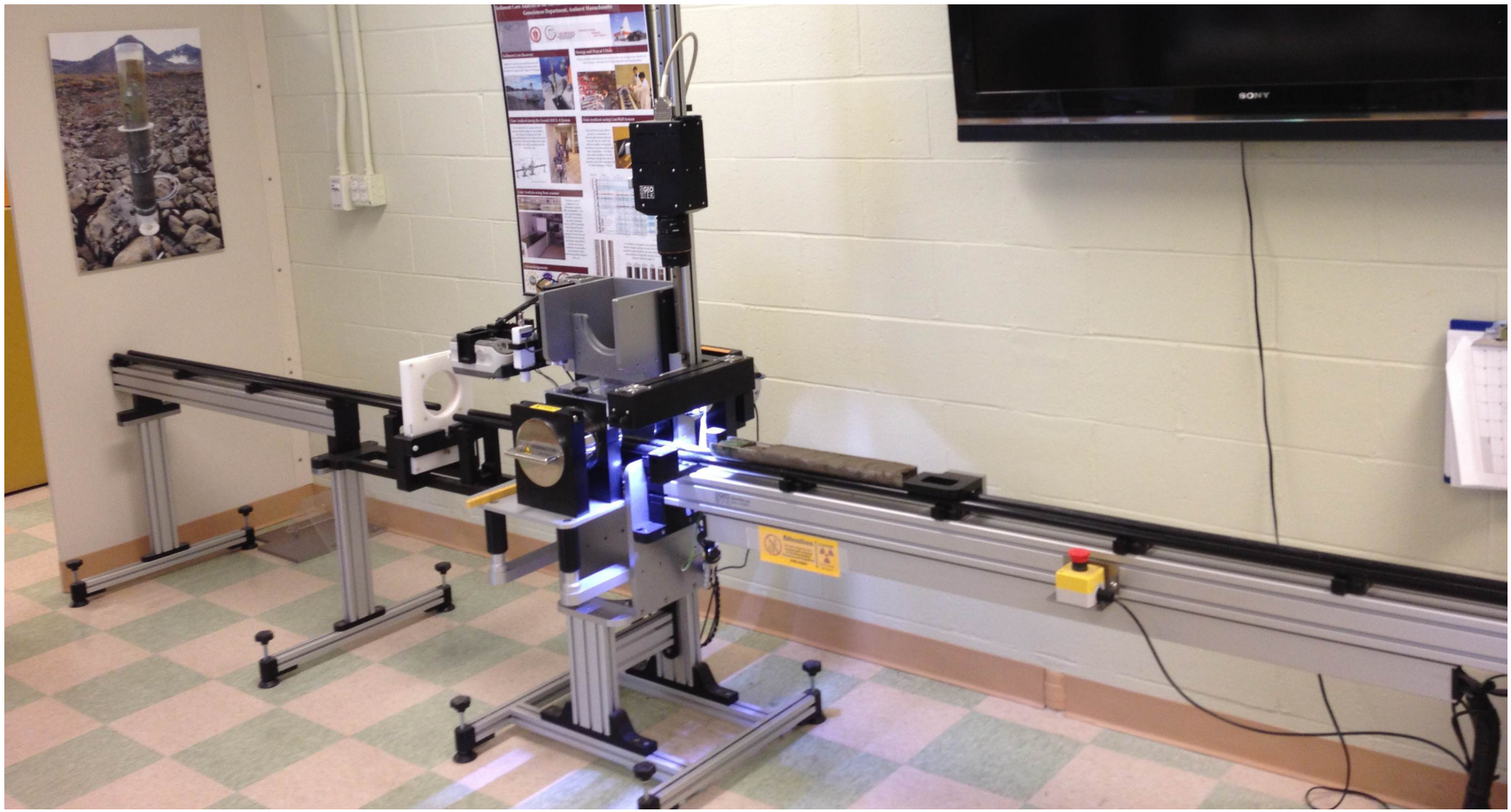

Figure 13 -A photograph of the Geotek Multi-Sensor Core Scanner in the University of Massachusetts Amherst Hartshorn Quaternary Laboratory. A core of similar length to core LH-4 is on the track.

periods of moraine stabilization on Svalbard defined by Werner (1993) and summer temperature reconstructions from alkenone unsaturation index (U^{K}_{37}) from Kongressvatnet from D'Andrea et al. (2012).

To determine whether or not the physical characteristics of the sediment record correlate well with the instrument record the sets of data were plotted side by side and against each other. The instrument data that was used was originally compiled by Kohler and was made available by Bates College Professor Retelle via Hampshire College Professor Steve Roof. The measurements included in the comparison were the physical characteristics of varve thickness and grain size and the instrumental record of average annual temperature, June, July, August (JJA) average temperature and total JJA precipitation. Temperature and precipitation data was compiled or calculated for every year from 1912 to 2010 except during the interval 1942-1944. During this time period precipitation data is not available and air temperature data is projected from mainland Norway measurements.

The relationship between climate and physical measurements was evaluated both visually, examining long-term trends in the data sets, and by running linear regressions between the two data sets and calculating an R^2 value. Actual climate measurements and varve thickness were plotted against each other with yearly data, with 5-year centered averages, and with 11-centered averages. In addition, climate data and varve thickness measurements were converted to anomalies using the equation Anomaly = (Mean-Measured Value)/(Standard Deviation) from Hardy et al. (1996). Mean normalized varve thickness was then compared to the weather data expressed as anomalies using the two comparison methods described above.

The comparison between LH-4 physical characteristics and the moraine stabilization study by Werner (1993) was of coarser resolution than the comparison to the instrumental record. Periods of warming (glacier retreat) and cooling (glacier advance) as defined in this study were compared on a decadal and century scale to the LH-4 varve thickness measurements. The final comparison with the D'Andrea et al. (2012) summer temperature reconstruction was of decadal scale due to the resolution of the reconstruction and potential similarities between climate conditions experienced at Kongressvatnet and conditions in Linnédalen.

After the climate signal contained in the LH-4 varve record was developed through an understanding of the Linnébreen proglacial system, and was partially verified by comparisons with two Svalbard paleoclimate reconstructions a picture of past climate conditions in Linnédalen was developed. This reconstruction was then placed in regional context through comparisons with various North Atlantic and Arctic climate proxy records.

Results

Visual Stratigraphy

Core LH-4 was comprised of laminated sediment with laminae between 0.25-2 mm thick. The laminae occur as couplets with a coarse-grained tan layer at the base that grades gradually into an overlying fine-grained dark grey layer In addition to the distinct couplets other laminated structures include distinct graded beds with silt-sand size particles fining upwards to silt-clay sized particles. The graded beds exhibit little color change from bottom to top in contrast to the lamination couplets. The intervals 0-13 cm, 16-31 cm, 31-35 cm, 35-43 cm, 43-45 cm and 45-49.5 cm contained lamination couplets without any visible change in lamination thickness or grain size. Of these intervals the laminations are well-defined from 16 cm to 31 cm and most poorly defined from 45 cm to 49.5 cm. The interval 13-16 cm is characterized by a series of thicker than average laminations. The graded bed layers occur in the core at depths of 31.7 cm, 44.2 cm, 46.3 cm, 49.6 cm, 53.7 cm, and 62.1 cm. Their thickness, shown in Table 1, range from 1.95 mm at 22.5 cm to 4.01 mm at 45.5 cm. A stratigraphic log and line scan image of short core LH-4 is shown in Figure 14.

Depth to Top of Graded Bed (cm)	Thickness of Graded Bed (mm)
22.5	1.95
30.1	2.24
31.7	2.41
35.3	3.00
38.7	2.48
45.5	4.01

Table 1 - This table show the depth to the top and thickness of the six graded beds indentified in core LH-4 through analysis of thin sections. The graded beds were identified by their coarser grain size, lack of color change from bottom to top, and the constant gradation of particle size.

The composition of core LH-Long is very similar to LH-4. The sediment record is primarily comprised of lamination couplets with a coarse-grained tan layer at the base that grades slightly into a fine-grained dark grey layer. Some intervals contain thicker lamination couplets with visibly coarser tan beds. The intervals 0-14cm, 17-31 cm, 31.5-35 cm, 35-44 cm, 44-46.5 cm, 48-50 cm, 55-57 cm, 60-64 cm, 66-69 cm, 74-76.5 cm, 78.5-82 cm, 82-84 cm, 87-96 cm, 96-105 cm, 105-111 cm, 111-113 cm, and 113-139 cm contain lamination couplets without any visible changes in lamination thickness, color or grain size. Of these intervals the lamination couplets are most distinct from 17-31 cm and least distinct from 31.5-35 cm and 113-139 cm. The interval from 14-17 cm contains a series of thicker lamination couplets. The graded beds layers found in core LH-4 can be identified

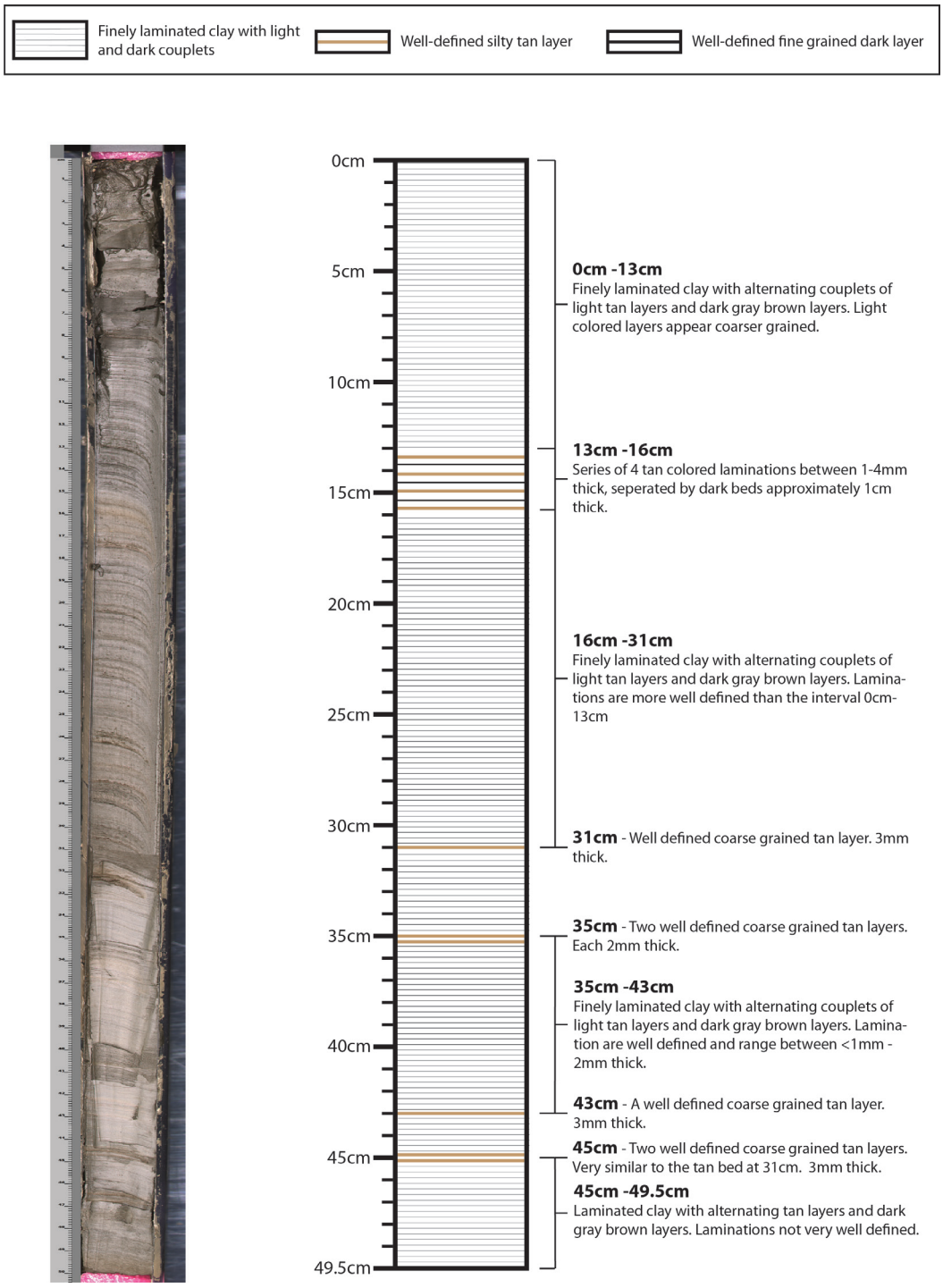

Figure 14 - A line scan image and schematic stratigraphic log of core LH-4. The line scan image was taken with the Geotek core scanner at the UMASS Hartshorn Quaternary Laboratory. The stratigraphic column highlights coarse grained layers that stood out visually.

visually at the same depth in core LH-Long. The intervals 50-55 cm, 57-60 cm, 64-66 cm, and 69-74 cm contain tan laminations that were >2 mm in thickness, some of which may be graded beds. Centered at a depth of 77 cm is the thickest single tan layer in the core at 3 cm thick. This layer is likely a very coarse grained graded bed. Centered at 85.5 cm is the thickest dark grey layer in the core at approximately 2.5 cm thick. At depths of 82 cm, 96 cm, 105 cm, 111 cm, and 113 cm are one or two (105 cm) coarse tan laminations 1-2 mm thick. A stratigraphic log and line scan image of core LH-Long is shown in Figure 15.

Density, %LOI, Grain Size and Magnetic Susceptibility

Dry density, bulk density, % Water, and % LOI measurements taken at 1 centimeter intervals along the length of core LH4, are shown in Figure 16. The data points are plotted at the midpoint of the subsampled interval. Bulk density values ranged from 1.33 g/cm^3 at 19.5cm to 1.94 g/cm^3 at 31.5 cm with an average of 1.58 g/cm^3. The greatest bulk density values were measured at 14.5 cm and 31.5 cm. The smallest bulk density values were measured at 1.5 cm, 19.5 cm, 22.5 cm, and 46.5 cm. An interval of high variability was present between 18.5 cm and 24.5 cm, while an interval of relatively constant values was present between 9.5 cm to 13.5 cm. Dry density values ranged from 0.87 g/cm^3 at 19.5 cm and 1.37 g/cm^3 at 31.5 cm. The average measured dry density was 1.08 g/cm^3. Peaks were seen at 14.5 cm, 21.5 cm, 23.5 cm and 31.5 cm. Low values were measured at 19.5 cm, 22.5 cm, 33.5 cm, and 46.5 cm. Intervals that record more substantial change include a decrease in values from 31.5cm to 33 .5cm, and from 45.5 to 46.5cm. % Water values ranged from 36.7% at 34.5 cm to 23.8% at 43.5 cm with an average value of 31.8%. % Water values exhibit the lowest variability from 0.5 cm to 31.5 cm. The interval from 31.5 cm to 34.5 cm is characterized by a steady increase in % Water. This is followed by a sharp decrease from 34.5 cm to 36.5 cm. % LOI values ranged from 6.4% at 36.5 cm to 9.3% at 8.5 cm with an average value of 7.8%. Measured % LOI values are characterized by intervals of relatively constant values separated by intervals of higher variability. Stable intervals include 8.5-13.5 cm, 16.5-22.5 cm, 24.5-28.5 cm, and 36.5-42.5 cm. Intervals of high variability include 0.5-8.5 cm, 13.5-16.5 cm, 22.5 cm-24.5 cm, 28.5-36.5 cm and 43.5-45.5 cm.

Figure 17 shows both mean and median grain size measurements from cores LH-4 and LH-Long. Data points are plotted at the midpoint of the subsampled interval. In core LH-4 subsamples were taken at 1 cm intervals and mean values ranged from 5.9 μm at 10 cm to 9.8 μm at 49 cm with an average of 7.4 μm. Median values ranged from 4.3 μm at 1 cm to 6.7 μm at 49 cm with an average value of 5.5 μm. Shifts in mean and median grain size are virtually the same along the length of the core. Peaks in mean and median grain size were measured at 3 cm, 12-16 cm, 34-36 cm, and 49 cm. Troughs occur at 9-10 cm, 17 cm, and 32 cm. The interval with the most stable mean and median values occurs from 25-30 cm. The interval with highest variability occurs from 43 cm to 49 cm. It is clear that the coarse tan laminations and turbidites identified in the core stratigraphy correspond to peaks in grain size.

The grain size analysis of core LH-Long is shown in Figure 17. Mean grain sizes ranged from

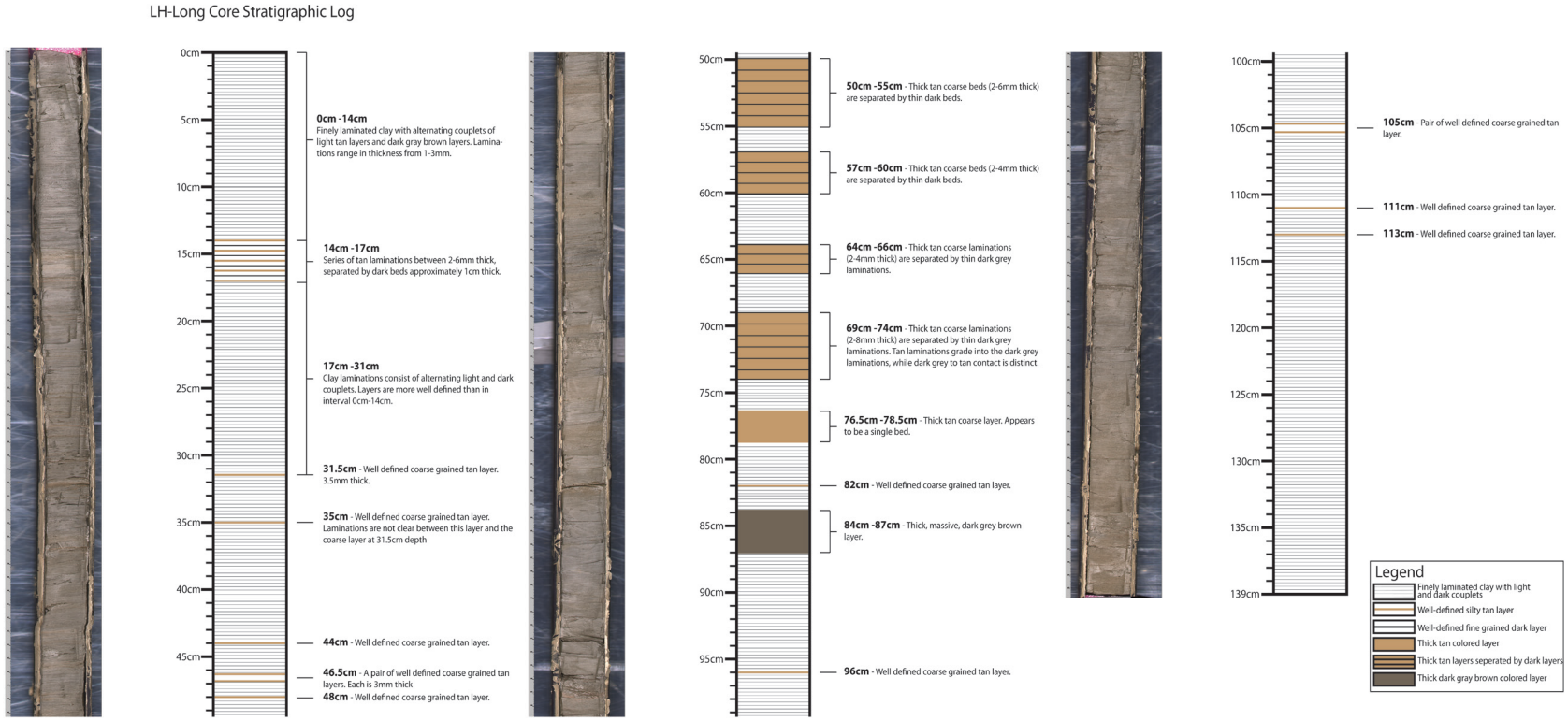

Figure 15 - A line scan image and schematic stratigraphic log of core LH-Long. The line scan image was taken with the Geotek core scanner at the UMASS Hartshorn Quaternary Laboratory. The stratigraphic column highlights coarse grained layers that stood out visually and thick dark grey layers.

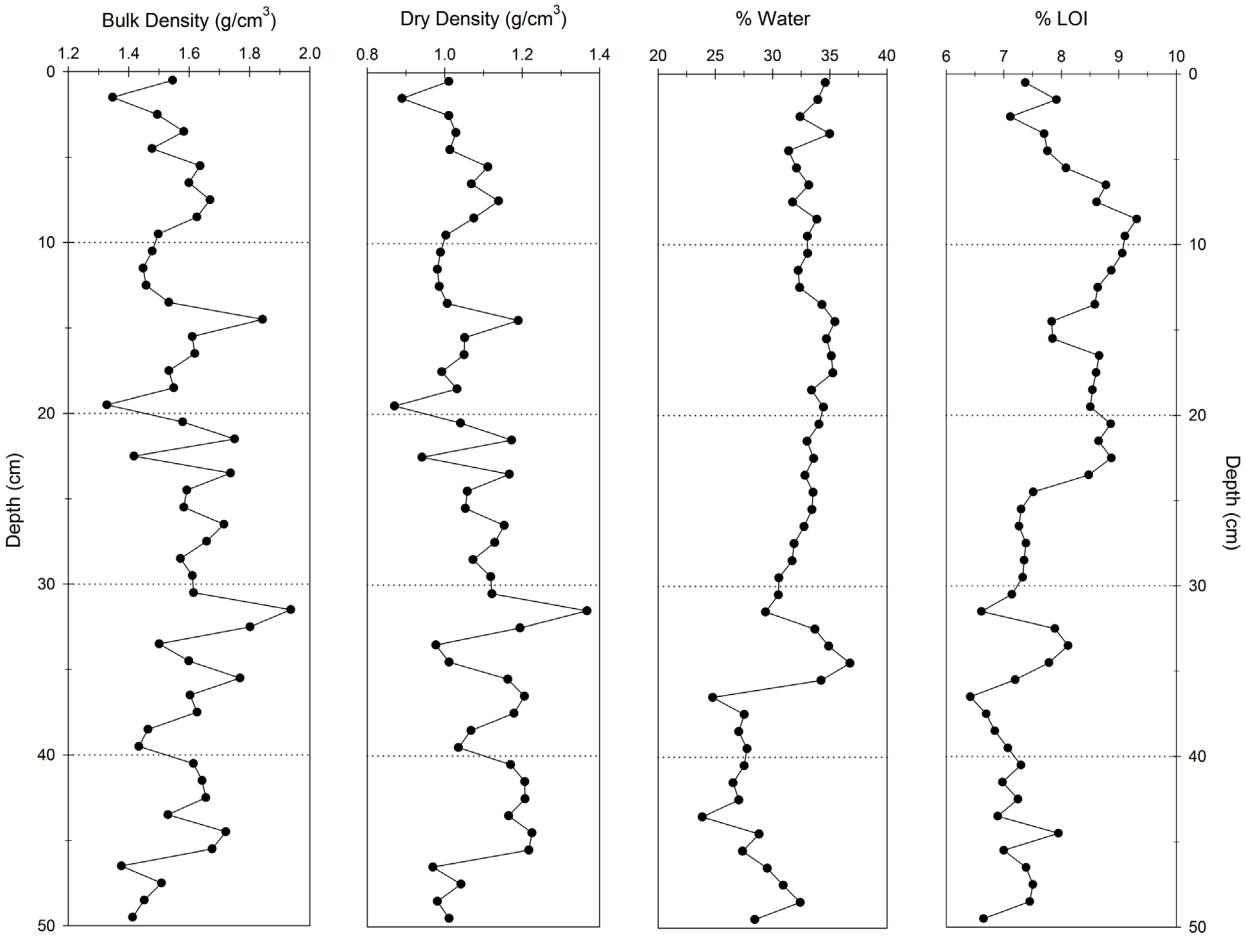

Figure 16 - Four plots illustrating bulk density, dry density, % Water and % LOI measured along core LH-4. Measurements were made from 1 cubic centimeter cubes of sediment. The data points are plotted at the mid-point of the subsampled interval. %LOI values remain low throughout the core and bulk density measurements vary through out the core.

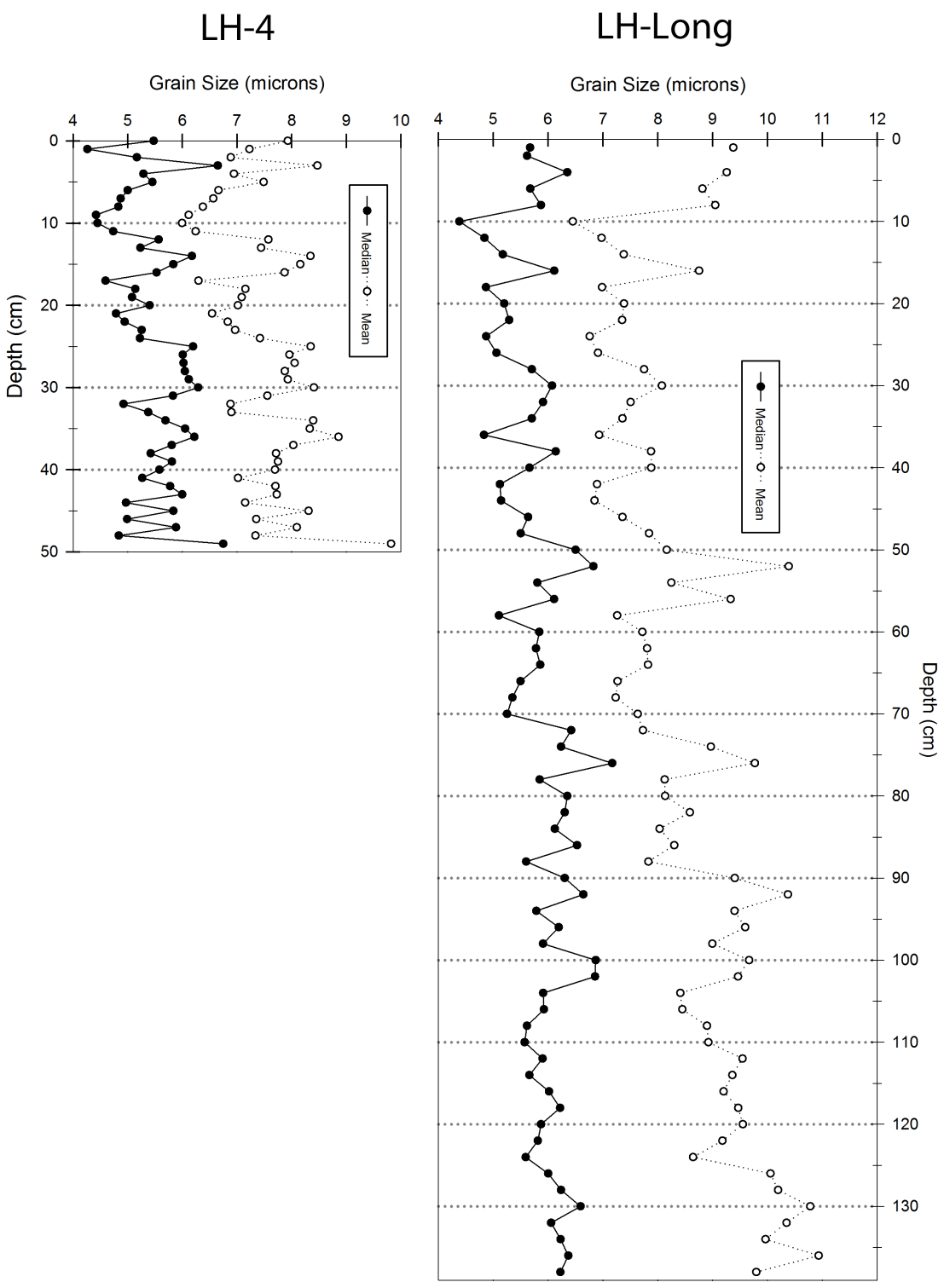

Figure 17 - Grain size measured from core LH-4 (left) and core LH-Long (right). Grain size was measured with a Beckman Coulter LS 13 320 Particle Size Analyzer at 1 centimeter intervals for core LH-4 and 2 centimeter intervals for core LH-Long.

6.5 μm at 10 cm to 13.2 μm at 2 cm with an average of 8.5 μm. Median values ranged from 4.4 μm at 10 cm to 7.2 μm at 76 cm with an average of 5.8 μm. Mean grain size values do not vary greatly along the core and are most stable from 104 cm to the base of the core. Median grain size mirrors trends in mean grain size along the length of the core but is slightly more variable. Peaks in median grain size occur in the intervals 50-56 cm, 72- 76 cm and 90-100 cm. It is clear that the tan marker beds and graded beds identified in the visual core stratigraphy align with peaks in both mean and median grain size.

Figure 18 shows magnetic susceptibility measured at 0.5 cm increments along core LH-4 and LH-Long. It is clear that relative changes in magnetic susceptibility are matched in both cores and the offset between the two cores stratigraphically is at most 2.5 cm. The absolute measurements are lower in core LH-4 than core LH-Long. The magnetic susceptibility measurements in core LH-4 ranged from 0 to 7 with an average of 2.48. The highest magnetic susceptibility values measured from core LH-4 occurred in the bottom 10 cm of the core. The magnetic susceptibility measurements in core LH-4 ranged from 1.9 to 8.6 with an average of 4.73. The highest magnetic susceptibility values measured from core LH-Long occurred from 123-140 cm.

Age Model and Varve Thickness

The upper 48 cm of core LH-4 is recorded in 10 thin sections due to the loss of material during thin section creation and the removal of sediment when the core was split and the end cap was removed. The reconstructed core from the thin section scans is show in Figure 19. The core contains 633 ± 25 lamination couplets. The uncertainty in the lamination couplet count was 4%. The measured thickness of these couplets ranged from 0.14 mm to 2.48 mm with a mean thickness of 0.73 mm and a standard deviation of 0.37 mm. The error associated with varve thickness measurements is 0.01 mm.

The results of plutonium geochronology performed on core LH-4 are shown in Figure 20. From a depth of 10 cm to 5 cm measured plutonium concentrations were below detectable levels. The departure from baseline levels occurs in the interval from 4.5-5.0 cm with a measurement of 0.07 Bq/kg $^{239+240}$Pu followed by greater departure in the interval from 4.0-4.5cm of 0.72 Bq/kg $^{239+240}$Pu. Plutonium levels increase up core and reach a peak of 7.39 Bq/kg $^{239+240}$Pu in the interval 3.0-3.5 cm. This peak is related to the deposition of sediment during the year 1963 (Ketterer et al., 2004). Above this peak plutonium levels drop towards the top of the core but remain at detectable levels.

Based on lamination couplet counts and measurement of lamination couplet thickness the interval containing the highest plutonium levels, 3.0-3.5 cm, contains a part or all of lamination couplets 41 through 50 counted from the top of the core. Assuming the lamination couplets were annual deposits the 49th lamination couplet was deposited in 1963. This couplet is located at a depth of 3.43 cm, within the peak plutonium interval, and can therefore be identified as sediment deposited in 1963. This confirms that the lamination couplets are varves (lamination couplets with annual periodicity). The 1952 onset, which occurs in the 4.0-4.5 cm interval provides additional evidence

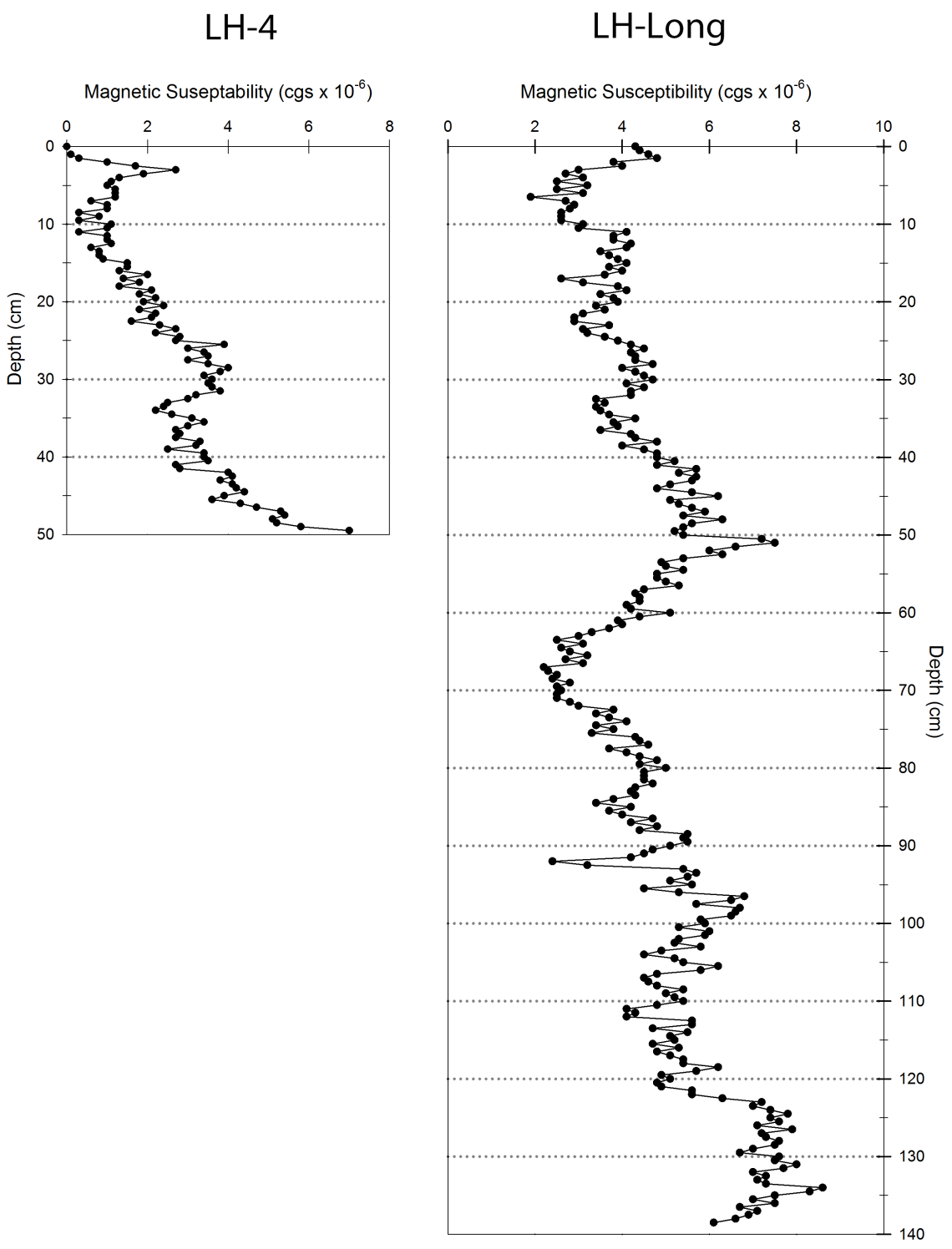

Figure 18 - Magnetic susceptibility measured from core LH-4 (left) and core LH-Long (right). Magnetic susceptibility was measured with the Geotek core scanner in the UMASS Hartshorn Quaternary Laboratory at 0.5 cm intervals.

Figure 19 - Core LH-4 reconstructed from thin section scans. The scans were aligned with the known 1 centimeter of overlap and marker beds. Thin sections 1a, 1b, and 1c all contain the sediment water interface. The total length of this composite core is 48 cm.

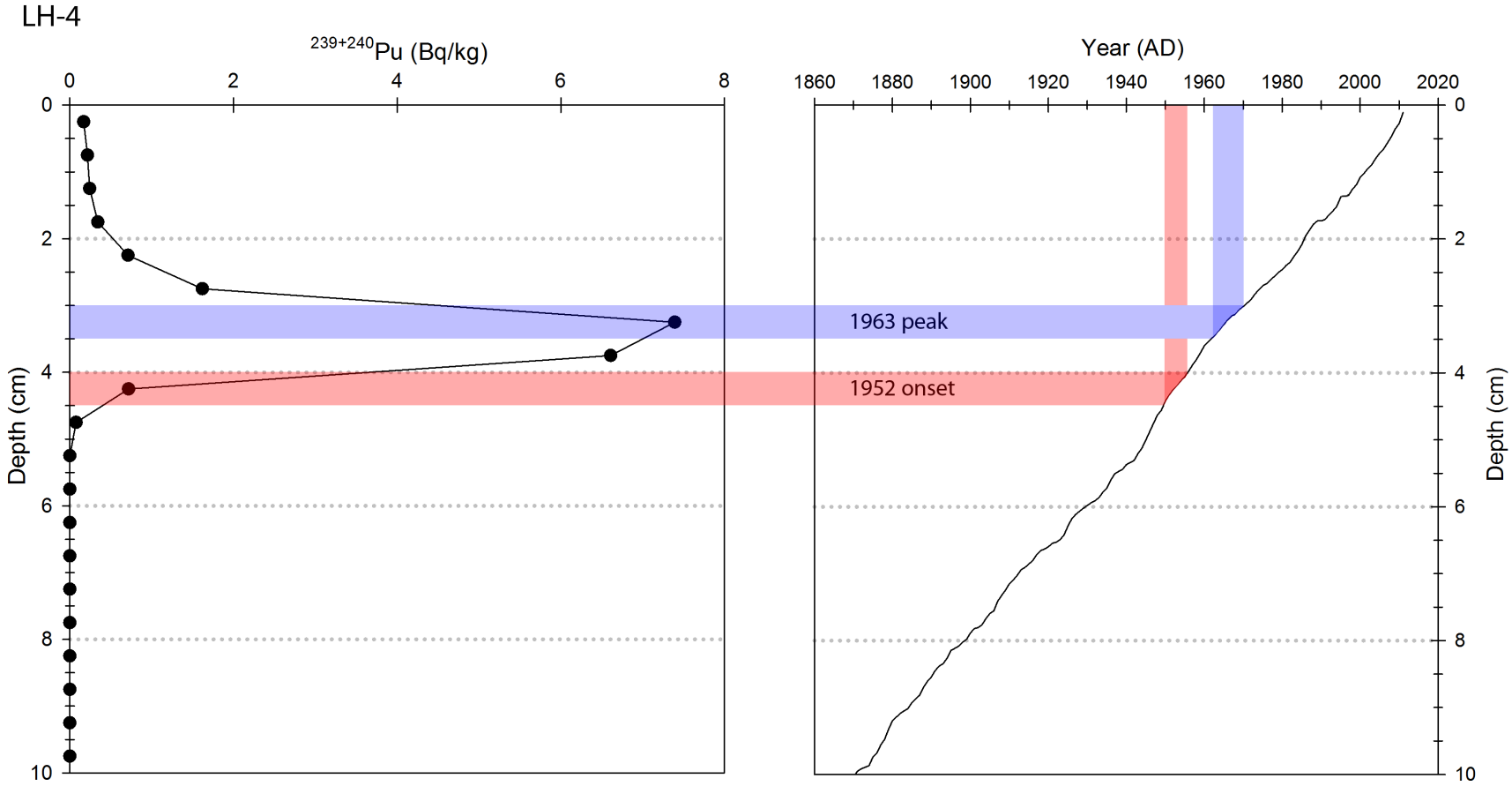

Figure 20 - The results of the plutonium age dating performed on core LH-4. The graph on the left shows plutonium concentration measured from 0.5 cm intervals along the core. The graph on the right shows year (determined from varve count) on the x-axis and depth on the y-axis. It is clear from these two graphs that the varves related to the years 1963 and 1952 fall within the corresponding subsampled interval defined by the plutonium curve.

that the sediment record is varved. This interval contains the 60th varve from the top of the core which was deposited in 1952. The relationship between the 1952 onset, the 1963 peak, and varve counts is also shown in Figure 20

With confirmation that the lamination couplets are varves, laminated couplet counts can be related to a specific year. This allows for the development of an age model for core LH-4. Figure 21, shows the LH-4 age model constructed from varve counts and measurements. Based on the age model core LH-4 contains a record reaching to at least AD 1402 and as far back as AD 1432. The intervals of highest sedimentation rate were AD 1750-1800 and AD 1500-1550. The interval of lowest sedimentation rate was AD 1800-1850.

Mean normalized varve thickness for the whole core and the interval from 1911-2010 is shown in Figure 22. The mean and standard deviation used to calculate mean normalized varve thickness were calculated from the interval shown in each plot . The trends in this plot are similar to those seen in the actual varve thickness measurements but the normalized values can be more accurately compared to normalized weather data and other temperature reconstructions. Overall, there is high variability in varve thickness throughout the sediment record. Trends are more easily seen in the 5-year running average, shown as a solid black line in the plot on the right side of Figure 22. The most prominent increases in varve thickness occur from AD 1750-1780, and AD 1850-1870. The greatest decreases in varve thickness occur from AD 1400-1450, AD 1550-1580, and AD 1790-1850. The interval with the lowest variability in varve thickness occurs from AD 1600-1700.

Climate Comparison

In order to determine the accuracy of the LH-4 climate signal the climate proxies analyzed in the core were compared to instrumental data from Svalbard Airport. This comparison also allowed for the development of the inital paleoclimate picture in Linnédalen based on the intervals of agreement between the instrument data and LH-4 varve thickness record.

Instrumental Record

To determine the accuracy of the LH-4 climate signal the climate proxies analyzed in the core were compared to instrumental data from Svalbard Airport and an array of Holocene climate reconstructions from Svalbard. Figure 23 shows a low-resolution comparison between grain size and precipitation. Grain size data is presented as the mean and median grain size for a 0.125 cm interval. The precipitation data represented by the bold red line is the average J,J,A precipitation during the years contained completely in the subsampled interval. Also shown on the graph is the 11-year centered average of J,J,A precipitation showing that the compartmentalized precipitation data is an accurate representation of the long term trends in precipitation. There is strong correlation between intervals of high mean and median grain size and intervals that contain years with high J,J,A precipitation. Linear regressions run between mean grain size and precipitation and median grain size and precipitation yield R^2 values of 0.8006 and 0.4669, respectively. The gap in precipitation data is

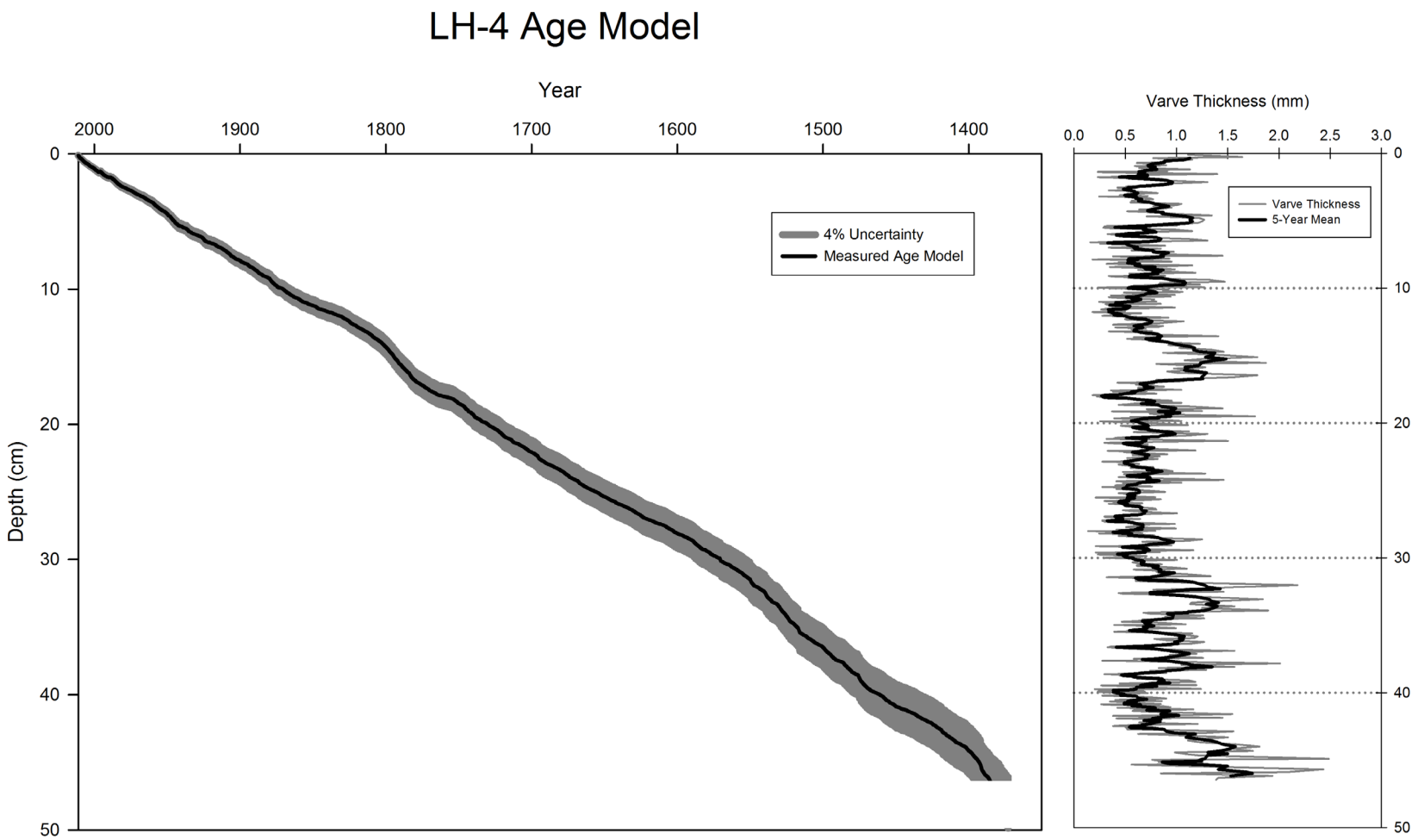

Figure 21 - The age model developed for LH-4 from varve counts and varve thickness measurements. The 4% uncertainty is derived from varying interpretation of sub-annual layers. Given this uncertainty the LH-4 sediment record reaches to at least AD 1432 and as far back as AD 1379.

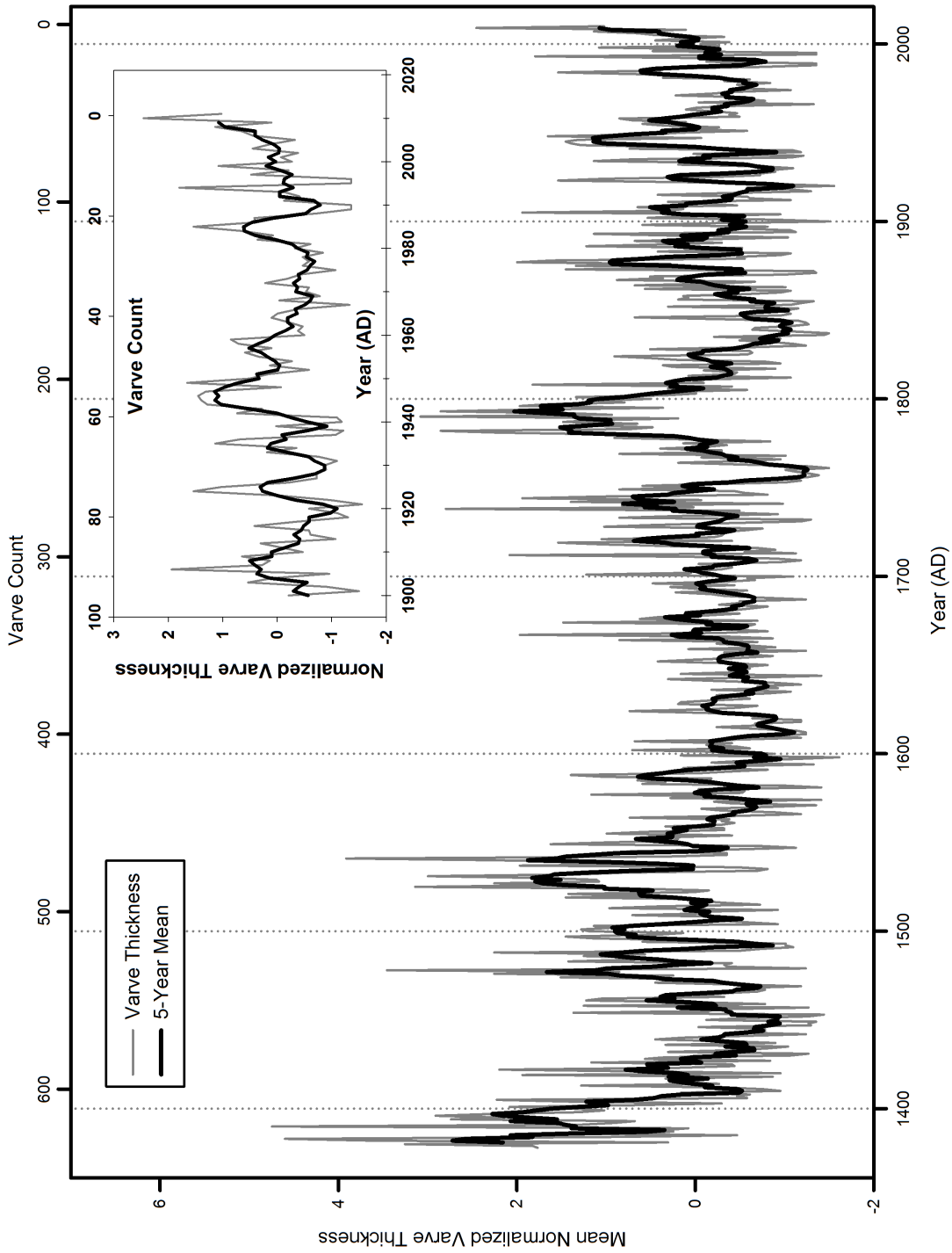

Figure 22 - Mean normalized thickness varve thickness measured from core LH-4 thin section scans. The varve count was related to year based on the age model shown in Figure 21. Inset: The mean normalized varve thickness over the past 100 years calculated with the 1911-2011 mean and standard deviation.

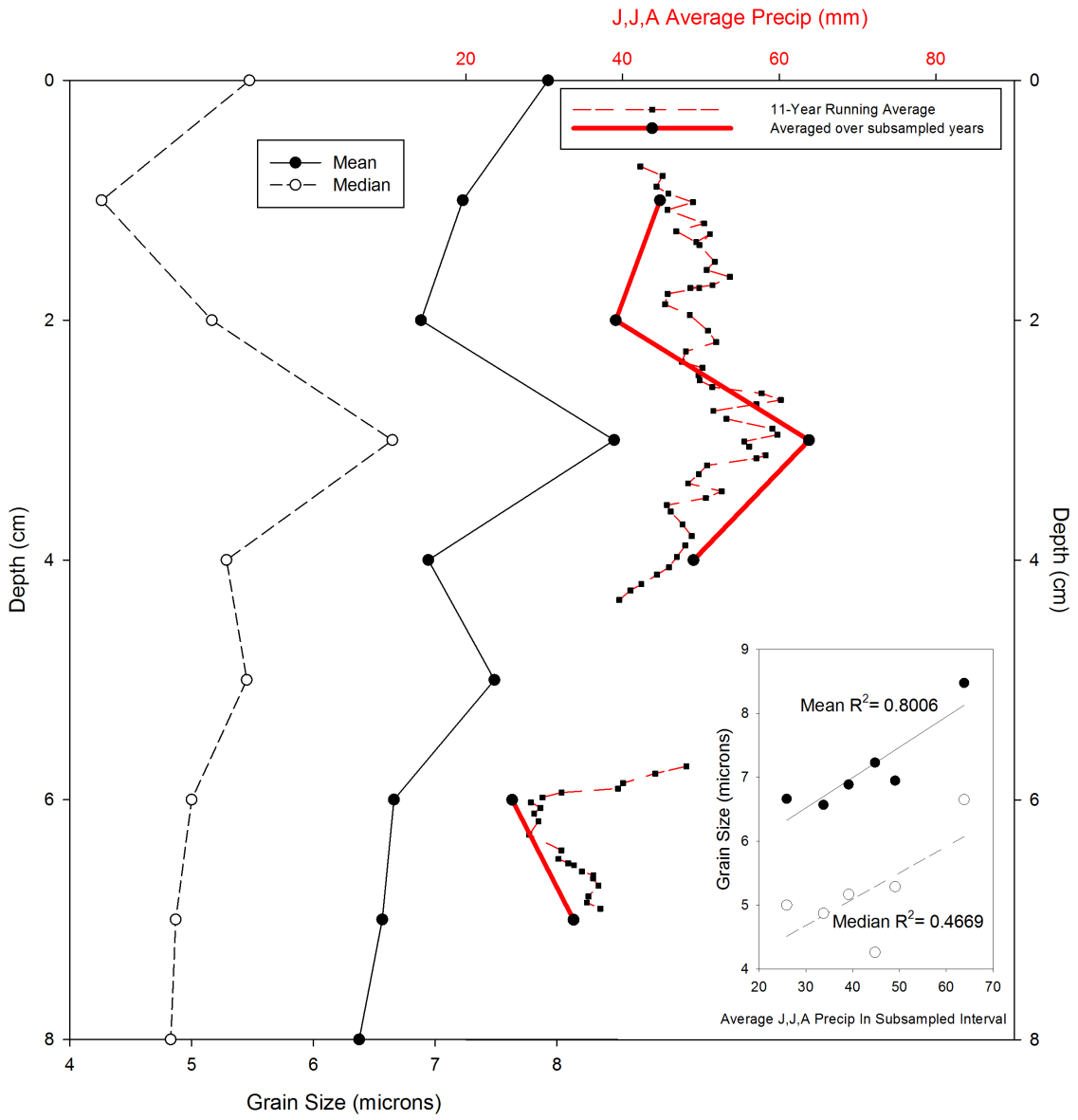

Figure 23 - LH-4 mean (solid black line) and median (dashed black line) grain size plotted next to total JJA precipitation averaged over the years contained in the subsampled interval (solid red line). Also shown is the 11-year center average of JJA precipitation (dashed red line), which illustrates that the comparmentalized precipitation data follows overall precipitation trends. Inset: Linear regressions between mean and median grain size and total JJA precipitation averaged over the years contained in the subsampled interval used for grain size analysis.

due to the lack of records in 1942, 1943, 1944.

Table 2 shows the degree of correlation between varve thickness measurements and weather data from the Svalbard Airport record expressed as an R^2 value. It is clear from the linear regressions that varve thickness correlates best with annual average temperature and shows no correlation with JJA average temperature and JJA total precipitation. There is an increase in the correlation between varve thickness and annual temperature from the 1 year to the 5-year and 11-year running averages .

Linear Regression R^2 Values	Varve Thickness Vs. Annual Average Temp	Varve Thickness Vs. JJA Average Temp	Varve Thickness Vs. Total JJA Precipitation
1 - Year	0.0505	0.0001	0.0004
5-Year Average	0.1546	0.0077	0.0078
11-Year Average	0.2320	0.0003	0.0158

Table 2 - This table contains the R^2 values of linear regressions between LH-4 varve thickness and the Svalbard Airport instrumental record from 1911-2011. The linear regressions were run on a year to year basis and with 5-year and 11-year averages. The strongest correlation exists between varve thickness average annual temperature. This correlation increases on longer time scales.

Table 3, shows R^2 values from linear regressions between mean normalized varve thickness (using the 1911-2010 mean and standard deviation) and climatic conditions expressed as anomalies. The R^2 values from linear regressions run between anomalies are higher for all compared fields than the between R^2 values derived from absolute measured values, shown in Table 2. The R^2 values for the linear regression between normalized varve thickness and annual temperature anomaly are higher than regressions run with the other climate parameters. There is increased correlation between normalized varve thickness and annual temperature anomaly from the 1-year to 5-year and 11-year running averages.

Linear Regression R^2 Values	Mean Normalized Varve Thickness Vs. Annual Average Temp Anomaly	Mean Normalized Varve Thickness Vs. JJA Average Temp Anomlay	Mean Normalized Varve Thickness Vs. Total JJA Precipitation Anomaly
1-Year	0.1133	0.0496	0.0355
5-Year Average	0.2279	0.0292	0.0025
11-Year Average	0.2479	0.0011	0.0001

Table 3 - This table contains the R^2 values of linear regressions between LH-4 mean normalized varve thickness and the Svalbard Airport instrumental record from 1911-2011 expressed as anomalies. The linear regressions were run on a year to year basis and with 5-year and 11-year averages. The strongest correlation exists between mean normalized varve thickness average annual temperature anomaly.

The correlation between the 11-year annual air temperature anomaly and 11-year mean normalized varve thickness can also be seen visually in Figure 24. It is clear in both plots that there are two periods of increase from approximately 1915 to 1942 and from 1967 to 2010 separated by

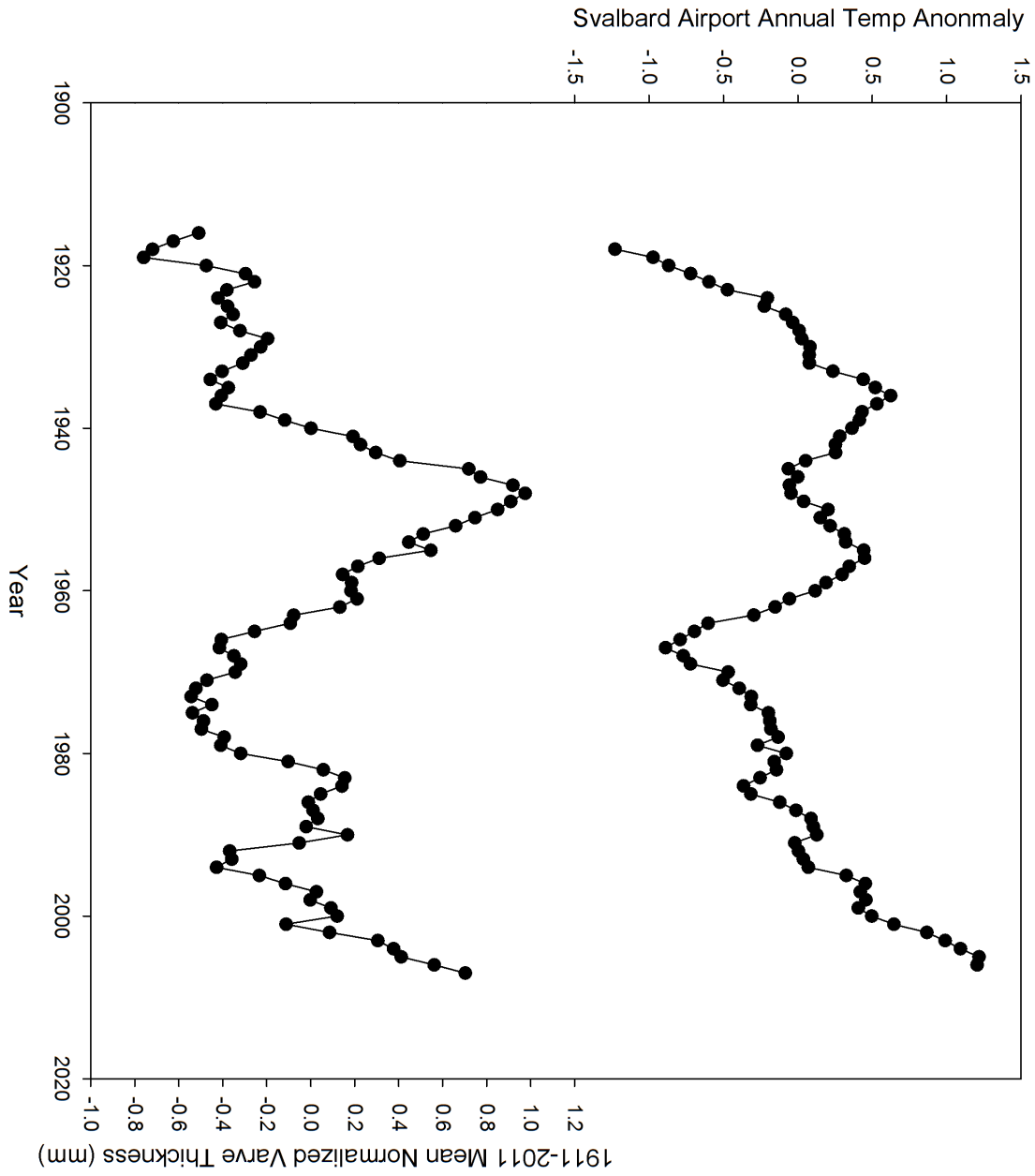

Figure 24 - The Svalbard Airpot annual air temperature anomaly plotted next to LH-4 mean normalized varve thickness from 1911-2011. There is strong correlation between the two records except in the interval from 1940 to 1950.

a period of decrease from 1942 to 1967. During the period from 1940 to 1950 the two plots do not appear to relate; annual temperature experiences a local minimum and varve thickness a local maximum during this interval. It is important to note that from 1942-1944 temperatures in the Svalbard Airport record were reconstructed from mainland Norway measurements (Nordli and Kohler, 2004).

Discussion

Previous analyses of the Linnévatnet sediment record have focused on interpreting the physical and geochemical properties of the sediment record to reconstruct long-term trends in glacier activity and climatic conditions in Linnédalen (Svendsen and Mangerud, 1997; Snyder et al., 2000). This study reconstructs past climate conditions in Linnédalen at decadal to century scale resolution by constructing a plutonium-verified varve chronology and using the physical characteristics of the sediment record as the primary climate proxy. This high-resolution analysis requires an understanding of how the Linnévatnet sediment records climatic changes in Linnédalen, an accurate interpretation of the sediment record, and a close comparison between the climate signal from Linnévatnet and other Svalbard paleoclimate reconstructions. Through this analysis a picture of climate conditions in Linnédalen over the past 600 years can be constructed and placed in regional climate context.

Age Model

A varve-based age model provides a high-resolution chronology for paleoenvironmental proxies within the sediment record that cannot be obtained with radiocarbon dates, tephrochronology or other dating methods (Ojala et al., 2012). The first step in developing a varve chronology is the confirmation of the annual periodicity of the lamination couplets in the sediment record (Ojala et al., 2012). The annual nature of the lamination couplets in Linnévatnet had been confirmed at site I and work has been done to confirm strong correlation between the lamination sequences found at different coring locations throughout distal basin and the eastern proximal basin (Nelson, 2010; Wei, 2010). Correlating these cores with confirmed varved records to LH-4 and LH-Long would have provided sufficient evidence that the sedimentary sequence at site H is varved. However in this study a more direct approach, plutonium age dating, was used to confirm the annual nature of the lamination couplets. This independent dating method has been used in many studies of varved sediment records because it provides two tie points for the age model at 1952 and 1963 (Ketterer et al., 2004; Ojala et al., 2012).

The results of the plutonium age dating, show in Figure 20, confirm that the laminations couplets in core LH-4 are varves. The 1963 peak in plutonium defined by Ketterer et al. (2004) occurs in the interval 3.0-3.5 cm that contains the 49th lamination couplet. The depth of the 1963 peak in core LH-4 is slightly deeper than the peaks found in cores analyzed by Nelson (2010) and Nereson (2010) which placed 1963 at 3.0 cm in a core from site I and at 2.9 cm in a core from site G, respectively.

In core LH-4 there is some uncertainty associated with the second tie point, the 1952 onset. Typically, the 1952 onset is related to the first data point that lies above baseline conditions measured deeper in the core (Ketterer et al., 2004). The plutonium curve, shown in Figure 20, has a value of 0.07 Bq/kg $^{239+240}$Pu associated with the interval 4.5 cm to 5 cm that shows an initial lift from baseline plutonium levels. However, based on varve counts and the interpretation of plutonium

dating cures in other varved sediment record studies the 0.72 Bq/kg $^{239+240}$Pu measurement associated with the 4.0 cm to 4.5 cm interval has been interpreted as the 1952 onset. This interpretation is based primarily on the plutonium-dating curve presented by Thomas and Briner (2009) from a varved sediment record in Baffin Island. In their study a plutonium value of approximately 0.8 Bq/kg $^{239+240}$Pu was interpreted as the 1952 onset (Thomas and Briner, 2009). This value is very similar to the 0.72 Bq/kg $^{239+240}$Pu value measured in Linnévatnet. This interpretation places the 1952 onset in the interval 4.0 cm to 4.5 cm, further aligning the plutonium dating curve to the varve chronology. In the future the resolution of the plutonium chronology could be improved with smaller subsampling intervals.

The lamination couplets in core LH-4 and LH-Long sediment record are consistent in their composition and overall thickness. This allows the varve chronology established in the upper 4 cm of the core to be extended through both cores. The lack of sub-annual layers in the sediment record allows for precise counting and identification of varves along both cores. The resulting LH-4 varve chronology has an uncertainty of 4% derived from the varying interpretation of sub-annual layers and errors associated measuring varves less than 1 mm thick. The 4% uncertainty lies just above the common range for varve-based chronologies with independent dating confirmation (Ojala et al., 2012), but would be higher in a core collected from a more proximal site in Linnévatnet with frequent sub-annual layering (Wei, 2010). The uncertainty derived from sub-annual layers could be lessened with a core from a more distal site. However, at these sites varve thickness is decreased and accurate interpretation of the sediment record is difficult (Nelson, 2010; Wei, 2010)

Long cores from the proximal western basin of Linnévatnet indicate that during periods when glaciers other than Linnébreen are present in the catchment the laminae in the sediment record are not varves (Svendsen and Mangerud, 1997). Further confirmation of the varve chronology via independent dating methods like tephrochronology (used at Kongressvatnet by D'Andrea et al., 2012) or ^{14}C dating (used at Linnévatnet by Svendsen and Mangerud, 1997 and Snyder et al., 2000) would further limit the uncertainty associated with the varve chronology and confirm that lamination couplets are in fact annual in deeper sections of the sediment record (Ojala et al., 2012). There is the potential to further constrain the age model by relating turbidite layers to earthquake events or turbidite layers in other lakes (Osleger et al., 2009). However, it is not certain that these layers are related solely to earthquake events and historical records of earthquakes throughout Scandinavia are sparse (Osleger et al., 2008; Wood and Woo, 1987).

The varve chronology developed from core LH-4 from AD 2011 to the late AD1300's, even with its uncertainty, is one of the highest resolution chronologies developed in Linnévatnet. This age model allows changes in the sediment record like graded beds, varve thickness, and other paleoclimate proxies to be related to a small temporal window of yearly to sub-decadal scale. An accurate chronology is essential when comparing paleoclimate proxies from Linnévatnet to other reconstructions and when developing a paleoclimate picture of Linnédalen in the Late Holocene.

The Climate Signal

After the development of an accurate varve chronology it is important to accurately record and interpret changes in the physical characteristics of the sedimentary record and determine how they act as paleoclimate proxies. The primary paleoclimate proxies used in this study, varve thickness and grain size, have been used as proxies in previous studies on Linnévatnet and have been shown to be closely tied to climate conditions in Linnédalen (Nelson, 2010; Wei, 2010; Svendsen and Mangerud, 1997). Before these proxies can be applied to cores LH-4 and LH-Long an understanding of how these proxies relate to climate in the setting of site H must be developed. This understanding has been fully developed for core LH-4. In the future this interpretation could be applied to core LH-Long further extending Linnédalen the paleoclimate reconstruction.

Varve Thickness

The % LOI data, shown in Figure 16, suggests that the concentration of organic sediment remains at low constant values throughout core LH-4. The three factors recorded in the % LOI measurements, primary production in the lake, sediment flux from the coal rich Billefjorden Group (Figure 5), and flux of water containing clay minerals, are not directly or inversely related to each other in the proglacial lake system. It is a safe assumption to conclude that these three factors have remained at low constant levels in Linnévatnet since AD 1379. This indicates that similar to most proglacial lakes on Svalbard the sediment record is dominated by clastic particles and changes in the physical characteristics of the sediment record are related to changes in the source of clastic material and sedimentation rate

Sedimentation rate in Linnévatnet is best recorded by varve thickness, a measurement that quantifies the amount of sediment deposited in a single year. In some lakes these measurements can be skewed by increased compaction as the sediment is buried by overlying sediment (Hughen et al., 2000). The bulk density measurements from core LH-4 indicate that compaction does not affect varve thickness in core LH-4. If compaction was a factor bulk density values would decrease steadily towards the top of the core (Thomas and Briner, 2009). The bulk density measurements illustrated in Figure 16 show a slight decrease in bulk density towards the top of the core in the upper 9 centimeters. However, there is a much larger decrease in bulk density from 30.5 cm to 19.5 cm. This confirms that variations in varve thickness throughout the record are tied only to sediment flux during a year. The findings from core LH-4 are consistent with Nelson's (2010) results based on mass accumulation rates calculated from a core collected from the more distal site G by Pratt (2006).

From the analysis of % LOI and bulk density measurements it is clear that varve thickness is primarily a function of the clastic sediment flux that settles at site H during a single year. Initial cores collected from site H in 2010 by Wei (2010) predominantly contained laminae related to annual sediment flux with infrequent sub-annual layering (Wei, 2010). These findings align with the low number of sub-annual laminae identified in core LH-4. The distance from Linnéelva (approximately 1.5 km) and depth at site H (40 meters) helps to ensure that the sediment deposited is not greatly

influenced by summer meltwater pulses and rainfall events (Wei, 2010). However, varves in cores recovered from site H are are generally sub-millimeter in thickness which can make identification of sub-annual layers difficult.

Overall, the thickness of the varves at site H was both beneficial and detrimental to reconstructing paleoclimate conditions through time. The benefit of sub-millimeter varves is that a 49.5 cm long universal core records 600+ years of the sedimentary record. The downside is that thin varves potentially limit both the temporal resolution of subsampling-based measurements (% LOI, grain size, etc.) and the correct identification of thin graded beds. The subsampling-based measurements were performed on an interval that contained between 2-8 years of sedimentation. This coarse resolution is not an issue when looking at decadal to century scale trends in the sediment record's characteristics but is a factor when an anomalous varve or graded bed can skew a measurement that is then applied to a series of years.

This effect of thin varves is most evident in grain size analysis performed on both cores. As seen in Figure 17 there is a strong correlation between spikes in grain size and the coarse grained varves identified visually and in thin section. In some intervals, like 13-16 cm, the entire interval is comprised of thicker varves that contain coarser grains. In this interval the grain size measurements are likely a good representation of grain size for all varves contained in the interval. However, at other locations where the subsampled interval contained a graded bed or a single coarse varve the grain size measurement is not a good representation of the grain size of each varve contained in the subsampled interval. These skewed measurements are a factor in all subsampling-based analyses in this study and also in measurements made with the Geotek scanner which are made at a single point spaced 0.5 cm apart and could skip over varves.

The interpretation of the LH-4 sediment record indicates that uncorrected varve thickness is an accurate measure of Linnéelva-derived sediment deposited during a single year, which based on the proglacial dynamics in Linnédalen can be related to summer temperature (Nelson, 2010; Wei, 2010). There is, however, a fair amount of uncertainty in this proxy as varve thickness can also be affected by biological productivity, precipitation, glacier position, and subglacial sediment storage (Thomas and Briner, 2009; Leonard, 1997). Measurements of % LOI from LH-4 confirm that biogenic sediment remains low throughout the core and bulk density values show that compaction is not a factor in varve thickness. The distal location of site H allowed for a long record with minimal sub-annual layering to be collected. This dampens the effect of recording,and thus, interpreting precipitation events compared to proximal coring locations (Wei, 2010). From air photographs and lichenometry it is known that Linnébreen lay at the Late Holocene maximum extent in the early 20th century and has since receded to its current position. The pre-20th century position of Linnébreen is unknown so the effects of glacier position on varve thickness cannot be quantified. Further evaluation of the accuracy of varve thickness as a summer temperature proxy based on comparison with other climate reconstructions is presented later in this study.

Grain Size

Changes in grain size throughout the 600+ year sediment record at site H can be attributed to changes in the grain size of the Linnéelva sediment flux, the introduction of sediment from other meltwater streams, large precipitation events and valley-side sources of sediment delivered to the lake shore by solifluction (Perrault, 2006). Changes in grain size of derived-Linnéelva sediment could result from many factors including changes in stream channel morphology, meltwater supply from the Linnébreen, and Linnébreen rock flour grain size. Due to the difficultly associated with tracking these factors back through time it is challenging to get a sense of if or how these factors have contributed to grain size shifts at site H. An idea of the role the other factors have on grain size at site H can be developed through an understanding of Linnédalen proglacial system.

Sediment flux from non-Linnéelva meltwater channels would result in increased grain size in site H varves because they would contribute previously unworked material into Linnévatnet's distal basin. The presence of these sediment sources is likely since there is evidence of additional cirque glaciers and large areas of perennial snowpack in Linnédalen during times colder than the present (Svendsen and Mangerud, 1997). Melt from these features in the summer would contribute sediment to Linnévatnet from sources located along the western valley wall, north of the Linnéelva delta. These alternate sediment sources would not result in sub-annual layering because the sediment influx would likely be synchronous with meltwater from Linnébreen, reworked from Solifluction lobes by wave action (Perrault, 2006). Unless the sediment arrived at site H as a gravity flow,the fine sediment from these alternate sources would mix in the water column and result in increased varve thickness and grain size.

The effect of precipitation on grain size can be determined by comparing precipitation data since 1911 from the Svalbard Airport and paleoprecipitation reconstructions to the grain size variations in core LH- 4, shown in Figure 23. This comparison is hindered slightly by the coarse temporal resolution of the grain size analysis and the potential for large precipitation events to result in sub-annual layering in the Linnévatnet sediment record (Wei, 2010). This sub-annual layering is most common at proximal locations in Linnévatnet where large precipitation events result in the formation of graded beds (Wei, 2010). However, the effect of large precipitation events on sedimentation at site H have not been tested. In the past ten years Linnédalen has experienced highly variable summer precipitation with some summers having minimal precipitation and others characterized by a single large precipitation event (Retelle, personal communication; Obermeyer, personal communication). However, there is no evidence of sub-annual layering or graded beds in the upper ten years of the site H sediment record. Extending this comparison back to 1911 the instrument record from the Svalbard airport contains three years (1937, 1972, 1981) with JJA precipitation of 100+ mm of precipitation (more than twice 45 mm average.) During these years there is no evidence of sub-annual layering in core LH-4. This relationship indicates that there has not been any precipitation events since 1911 of the magnitude required to form a graded bed at site H. There is, however, increased grain size associated with these large summer precipitation years in the sediment record. In fact, the comparison between JJA precipitation values and grain size in

the upper 8 cm of core LH-4, shown in Figure 23, suggests that large precipitation events result in increased grain size in site H varves. It is not sufficient to relate all precipitation events since AD 1379 to coarsening of a varve and not the formation of a graded bed because of this relationship established in the upper 8 centimeters of the core. If precipitation was higher during the Little Ice Age as suggested by D'Andrea et al. (2012) then it is possible that large summer precipitation events would be in excess of 100 mm and could result in graded beds at site H.

In conclusion, grain size is a more complicated proxy than varve thickness as it can be related to general Linnéelva sediment flux, alternative sediment inputs and large precipitation events. In the upper part of the core it is clear that precipitation is the dominant factor in determining grain size as indicated by the strong correlation between grain size and precipitation. These findings are consistent with grain size analysis related to precipitation as determined by Obermeyer (personal communication).

Graded Beds

The graded beds in the site H sediment record provide paleoclimate insight and can be accurately dated by the varve chronology they interrupt. The graded beds in the core LH-4 are characterized by increased grain size compared to the typical varve sequence and a thickness of 1.5-4.0 mm. Possible causes of graded beds include additional sediment sources, large precipitation events, and slumping events (Wei, 2010). A comparison between grain size fluctuations in core LH-4 and precipitation records suggests that even the largest summer precipitation events in the instrumental record which could be recorded as graded beds at more proximal sites do not result in graded beds at site H. This is not enough evidence to suggest that even larger precipitation events in the past would not have deposited graded beds in Linnévatnet's distal basin, and precipitation could be responsible for the graded beds found deeper in the core. The most likely mechanism for graded bed formation is slumping or landslide events. These events are episodic in nature and would input coarse grained material into the distal basin (Wei, 2010). Linnédalen has steep slopes on both the eastern and western sides and slope or active layer failure is common in the flatter terrain in the northern end of the valley (Farnsworth, personal communication).

In other proglacial lakes graded beds have been interpreted as the result of landslide or slumping events (DeWet, 2013; Leonard, 1997). Slope instability is typical in basins with steep walled terrain and landslide can be a major contributor of large sediment pulses into a lake (DeWet, 2013). Slumping commonly occurs in lakes with steep bathymetry when sediment build up crosses a threshold and slumps into a deep basin (Osleger et al., 2009). In Hector Lake, a proglacial lake with similar bathymetry to Linnévatnet, turbidites have been attributed to surge currents caused by slumping events (Leonard, 1997). Due to the similarities between Linnévatnet and Hector Lake the graded beds in Linnévatnet are most likely the result of slumping events, although their sporadic nature suggests they are triggered by a catastrophic event such as an earthquake and not the collapse built up of sediment.

In conclusion, the graded beds in Linnévatnet are most likely related to infrequent slumping

events although the possibility of anomalous summer precipitation cannot be completely eliminated. It is not likely that the slumping events are related to climate conditions in Linnédalen as they are probably connected to the active tectonics of the Mid-Atlantic Ridge running through in Fram Strait. Future mineralogic analyses could constrain the source of material contained in the graded beds and perhaps provide insight into their mechanism of formation (Perrault, 2006).

Comparison with Climate Records and Reconstructions

The climate signal recorded by varve thickness in the site H sediment record has been determined through an understanding of the Linnédalen proglacial system. The accuracy of this climate signal can be evaluated by comparing it to other paleoclimate reconstructions in Svalbard. If the climate signal determined from Linnévatnet is accurate, one would expect good correlation with proximal constructions and agreement with long-term trends in regional reconstructions. Meaningful comparisons with other paleoclimate reconstructions are reliant upon having an accurate chronology (Ojala et al., 2012). The LH-4 chronology is fairly high resolution but contains 4% uncertainty associated with varying interpretations of sub-annual layering. Given this uncertainty and the increased correlation between varve thickness and climate records on longer timescales comparisons were made between decadal and century length trends in the records.

Instrumental Record

The instrument record from the Svalbard Airport provides a high resolution record of climate conditions in Longyearbyen. This weather station, located further inland on the southern coast of Isfjorden, commonly records temperatures slightly warmer than those experienced in Linnédalen (Nordli and Kohler, 2003). However, strong correlation with this record has been used to confirm the accuracy of summer temperature reconstructions at Kongressvatnet and Linnévatnet (D'Andrea et al., 2012; Nelson, 2010). Due to the uncertainty inherent in the varve-chronology it is not expected that weather parameters and climate proxies in the record align on a year to year basis. Good correlation would be expected between related variables on longer timescales (Leonard and Reasoner, 1999).

The results of linear regressions run between Svalbard Airport weather data and LH-4 varve thickness, shown in Table 2, indicate weak correlation between LH-4 mean normalized varve thickness and both summer precipitation and summer temperature anomalies on yearly to decadal timescales. With respect to precipitation this lack of correlation suggests that large precipitation events do not result in large increases in varve thickness at site H. This indicates that precipitation is not a major factor in varve thickness and, therefore, varve thickness should be a good indicator of Linnéelva sediment flux throughout the record. The lack of correlation between summer precipitation and varve thickness confirms the grain-size-based precipitation analysis outlined earlier in this section. The result from this study is opposite of previous work by Nelson (2010) who found good correlation between JJA precipitation and varve thickness at site I.

The weak correlation between summer temperature and varve thickness could potentially be

the result of differences in summer temperature between the two locations. Comparing the summer temperatures between Linnédalen and Svalbard Airport in 2005 and 2010 it is clear that the JJA temperatures in Linnédalen are cooler than the Svalbard Airport, as shown in Table 4. Two years of data is not sufficient to make an estimate of how Linnédalen temperatures differ from those at Svalbard Airport, but they are an indication that climate conditions vary between these two locations.

Year	Linnédalen JJA Temp (°C)	Svalbard Airport JJA Temp (°C)
2010	4.39	4.97
2005	5.20	6.17

Table 4 - The average JJA temperature recorded in Linnédalen and Svalbard Airpot in 2005 and 2010. In both years Svalbard Airport temperatures are higher.

The strongest correlation exists between mean normalized varve thickness and annual air temperature anomaly. The R^2 value is small for the year to year comparison, but increases with 5-year and 11-year averages. This suggests that varve thickness and annual air temperature are increasingly correlated on longer timescales. Increased accuracy of a varved sediment record on longer timescales is common when comparing varve chronologies to climate information (Leonard, 1997; Nelson, 2010). The increased accuracy is due to both the diminished effect of errors in the age model on longer timescales and the complexities of the proglacial system which can affect the varve record in unexpected ways on a year to year basis (Leonard, 1997).

Further analysis of the relationship between varve thickness and annual air temperature shows that the correlation between these two variables could be stronger except for the negative correlation between the two variables from AD 1940-1950. It is possible that increased precipitation during this time in at Svalbard airport during this interval could be responsible for the increase in varve thickness at the same time as this drop in temperatures. Through the rest of the record this relationship between precipitation and varve thickness is not seen but the gap in the precipitation data over this interval prevents this explanation from being fully eliminated.

In conclusion, there is good correlation between Svalbard Airport annual air temperature and varve thickness. This correlation would likely increase if a long record of temperature from Isfjord Radio was available and if the role of precipitation on varve thickness could be precisely determined.

Moraine Stabilization

In the past 1,000 years there have been two periods of moraine stabilization associated with the Little Ice Age in Svalbard (Werner, 1993). The first occurred approximately 650 years ago and the second occurred in the past few centuries (Werner, 1993). These periods of moraine stabilization provide a good indicator of how Linnébreen mass balance has varied over the last 1,000 years. A comparison between these periods of known glacier recession and the varve thickness record from

Linnévatnet serves to both confirm varve thickness as an indicator of Linnébreen glacier mass balance and to develop a paleoclimate picture of Linnédalen since AD 1379.

The two periods of moraine stabilization are plotted in green against LH-4 varve thickness measurements in Figure 25. The first period of moraine stabilization 650 years ago is followed by above average varve thickness for 33 of the next 35 years. Based on the interpretation of factors that affect varve thickness at site H it is clear that the increased varve thickness during this interval is reflecting increased sediment flux from Linnéelva, a result of the negative mass balance of Linnébreen.

The second interval of moraine stabilization on Svalbard is loosely constrained to the past few centuries due to the variability of glacier conditions on Svalbard (Werner, 1993). Post-Little Ice Age glacier retreat can be narrowed for Linnébreen through analysis of air photos from 1936 and 1995-present, shown in Figure 26. From the 1936 air photo it is clear that the glacier terminus lies at the Little Ice Age moraine marking its maximum Late Holocene extent (Svendsen and Mangerud, 1997). Based on the present day position of the glacier terminus there has been significant retreat of Linnébreen from 1936 to the present. This period of retreat is reflected in the LH-4 varve record as two periods of general increased varve thickness from 1936-1945 and 1980-2011, and a steady decrease in varve thickness from 1945-1980.The two periods of increasing varve thickness are synchronous with significant warming periods in the Svalbard Airport temperature record and the decrease in varve thickness is synchronous with a significant cooling trend in the instrument record (Førland et al., 2011). The varve record and instrument record suggest that glacier retreat was highest from AD 1936-1945 and from AD 1980 to the present and slowed from AD 1945-1980.

Based on air photo evidence and the established relationship between annual air temperature, Linnébreen mass balance, and varve thickness it appears that changes in varve thickness from AD 1936 to the present are accurate indicators of climate conditions in Linnédalen on decadal timescales. The strength of this relationship diminishes back through time as the uncertainty in the varve record increases and the state of glaciers and climatic conditions in Linnédalen is less understood.

Lake Kongressvatnet Reconstruction

A summer temperature reconstruction by D'Andrea et al. (2012) from Kongressvatnet located 2 km to the southeast of Linnévatnet provides another paleoclimate record to compare to the LH-4 varve thickness record. The 1,800 year reconstruction, based on alkenone paleothermometry, defines two periods of warmest summers, from AD 1750 to 1780 and from AD 1987 to 2009. These periods shown in red in Figure 25 occur synchronous with two of the most substantial varve thickness increases in the LH-4 record. The implications of this alignment between the two reconstructions are twofold. First, it would be expected that due to the proximity of Kongressvatnet to Linnévatnet the climate record from Kongressvatnet would align with the climate signal in core LH-4. The alignment of these records over the two intervals provides additional support, beyond the evidence provided in previously, that LH-4 varve thickness is an accurate proxy of summer temperatures. Second, the agreement between the two records suggests that the periods from AD 1750 to 1780 and from AD 1987 to 2009 were times of high summer temperatures in Linnédalen.

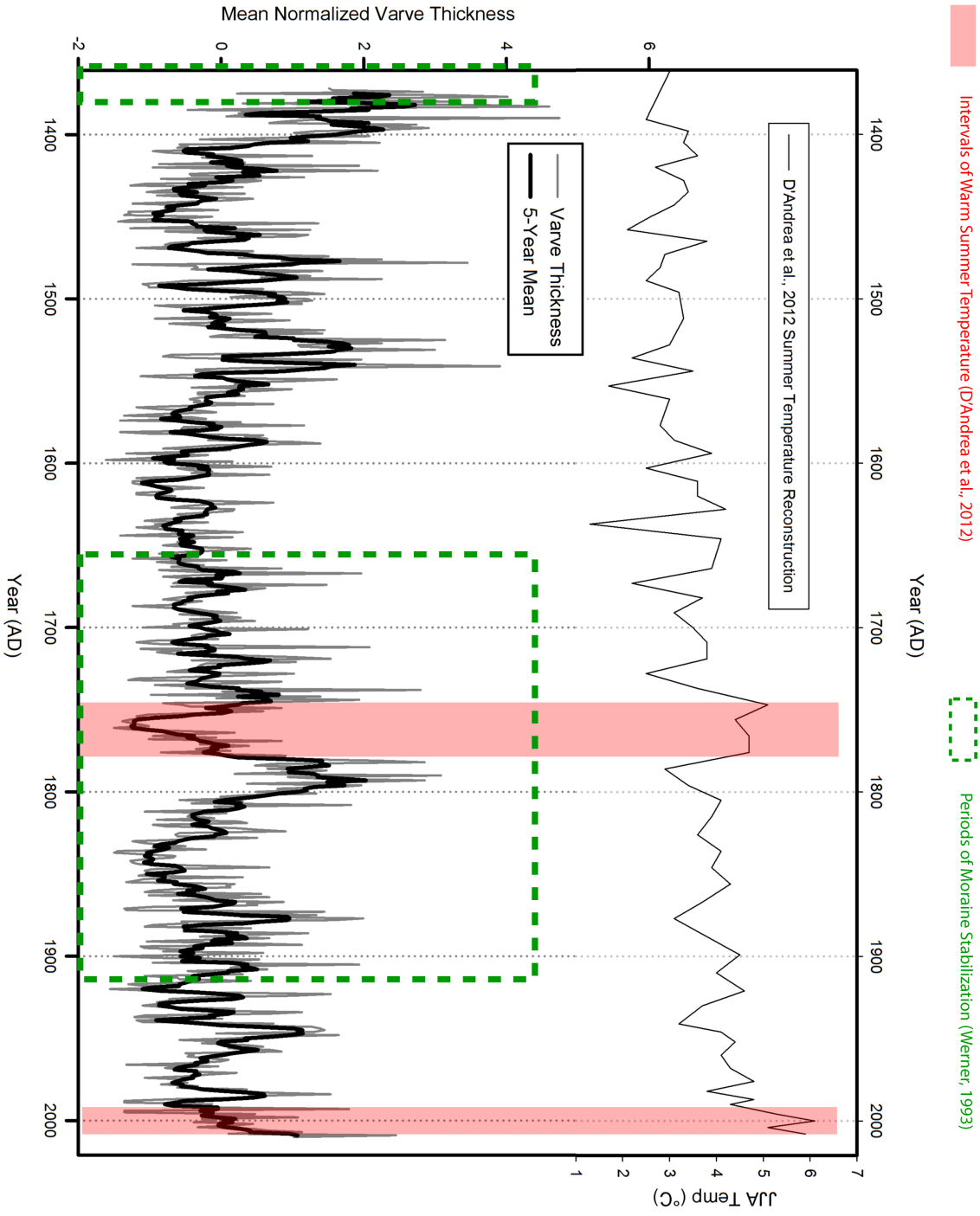

Figure 25 - Periods of moraine stabilization (Werner, 1993) and warmest suumer temperatures (D'Andrea et al., 2012) overlain on mean normalized varve thickness. Following the first period of moraine stabilization 650 years ago varve thickness remains above average for 33 of the next 35 years. The second period of moraine stabilization in the past few centuries is more accurately defined for Linnébreen by air photos in Figure 26. The two periods of warmest summer temperatures from the D'Andrea et al. (2012) summer temperature construction are shown in red. These two intervals both relate to increases in varve thickness.

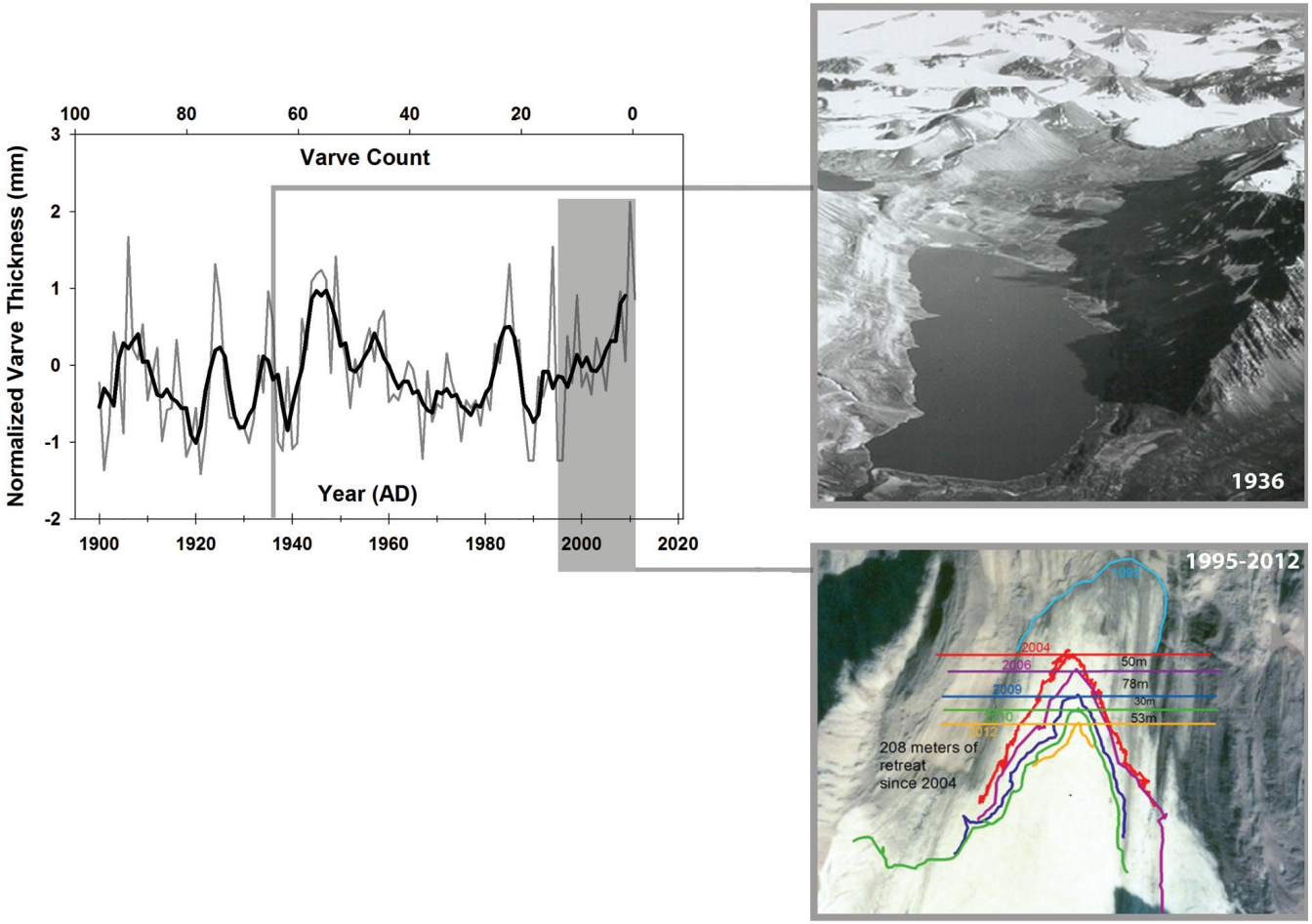

Figure 26 - Air photos from 1936 of Linnédalen (Norsk Polarinstitutt) and from 1995 of Linnébreen (Svalbard REU) compared to LH-4 mean normalized varve thickness. Tracks of Linnébreen glacier termini from 1995 to 2012 are traced on the lower air photo.

Throughout the rest of the LH-4 varve thickness record increased summer temperatures from Kongressvatnet do not relate well to increases in varve thickness. It is possible that these smaller temperature increases were not high enough or long enough to result in increased varve thickness at site H. Further interpretation regarding the alignment of the two records is difficult because the Kongressvatnet record is of relatively low temporal resolution but there is low uncertainty associated with the alkenone summer temperature proxy and the tephra-constrained age model. The LH-4 varve thickness record on the other hand is of higher temporal resolution but varve thickness is not closely as closely tied to summer temperature due to the complexity of the proglacial system (Thomas and Briner, 2009). Overall, the comparison between these two records has shown that the climate signal recorded in Linnévatnet at site H and climate signal from Kongressvatnet sediment record are in agreement during periods of high summer temperatures. This alignment has been used in part as further confirmation of LH-4 varve thickness as a summer temperature proxy and has provided evidence that the periods from AD 1750-1780 and AD 1987-present are times of high summer temperatures in Linnédalen.

Late Holocene Climate Conditions in Linnédalen

Through careful analysis of the site H sediment record and an understanding of the proglacial processes in Linnédalen a climate signal, based primarily upon varve thickness, has been developed from core LH-4. This climate signal, combined with the plutonium-verified varve chronology, provides insight into paleoclimate conditions in Linnédalen since AD 1379. Comparisons between this climate signal and other paleoclimate reconstructions have served to both verify the climate signal and provide initial estimates of periods of warm summer temperatures in Linnédalen. Additional Late Holocene paleoclimate projections can be made from the LH-4 varve thickness record based on the appearance of these confirmed warm periods in the Linnédalen's climate history. Given the uncertainties associated with the varve chronology and the unresolved effect of precipitation, glacier position through time, and subglacial sediment production on varve thickness, the timing of the projections are defined by decade. The final paleoclimate picture of the Linnédalen during the Late Holocene has been placed into regional context through comparison with regional and hemisphere-scale climate trends during this period.

The previous comparisons between LH-4 varve thickness and the moraine stabilization record, air photographs, and the Kongressvatnet summer temperature reconstruction resulted in the confirmation of three periods of warm summer temperatures in Linnédalen. The three periods refined to best match changes in the LH-4 varve record are shown in red on Figure 27. These intervals of warm summer temperature, from AD pre-1379 to the late 1390's, from the AD 1760's-1790's, and from AD 1980's-present, are represented in the LH-4 varve record as sustained above average varve thicknesses or by sustained increases in varve thickness. Based on the interpretation of a warm period in the intervals listed above an additional warm period, not identified through the reconstruction comparisons, can be defined from AD 1850's-1870's. This period, also shown in red in Figure 27, relates to a substantial increase in varve thickness and does correspond to the end of a warm temperature interval in the Kongressvatnet reconstruction (D'Andrea et al., 2012).

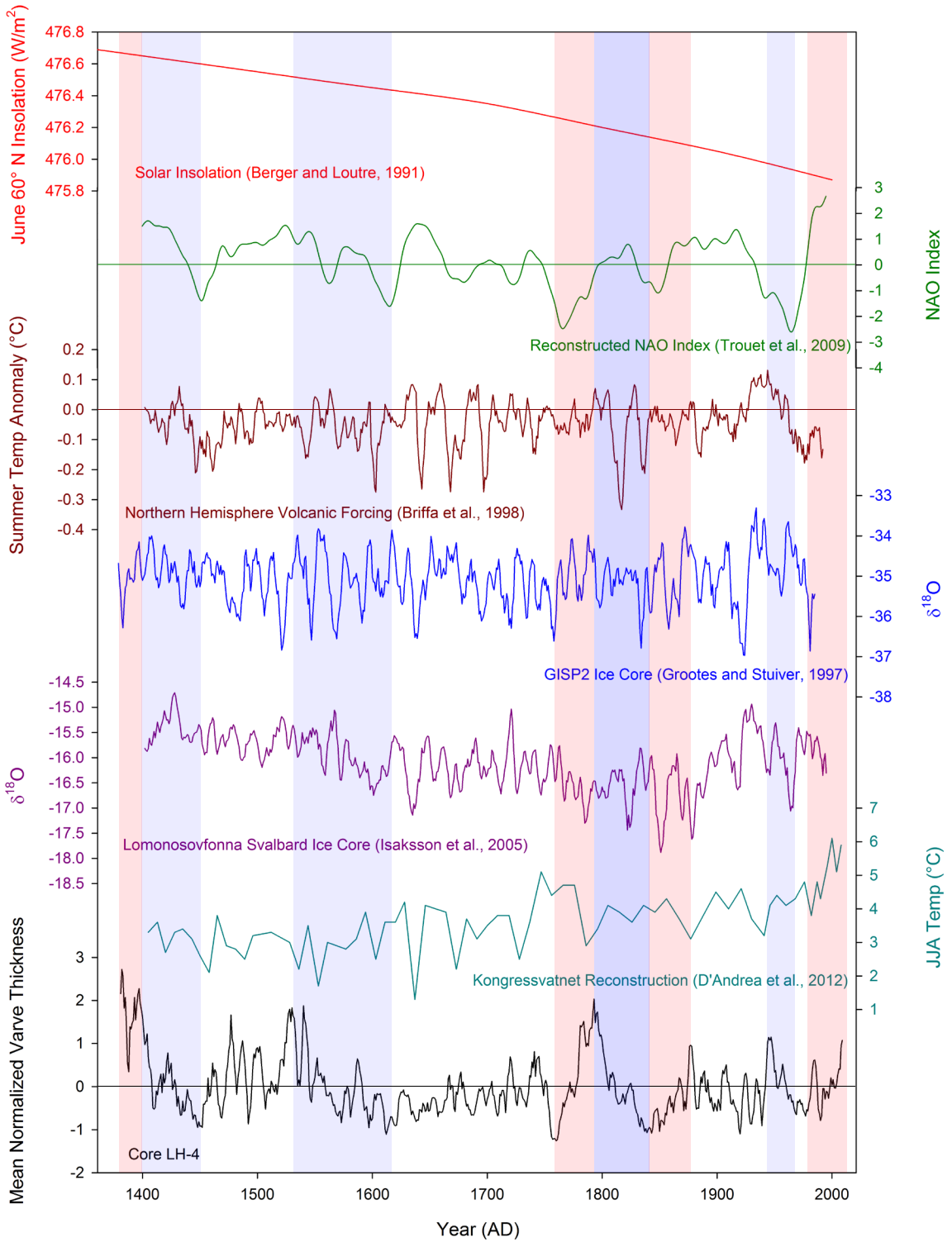

Figure 27- A graph of proxy based Arctic and North Atlatic climate records from pre-1400 to 2011 plotted next to LH-4 mean normalized varve thickness. The reconstructions increase in scale from bottom to top. The warm and cool intervals in Linnédalen defined in this sudy are shown in red and blue, respectively.

Cool summer temperatures in Linnédalen result in steady decreases in varve thickness or periods of below average varve thickness in the LH-4 sediment record. This relationship is based on the understanding of proglacial process developed in this study and by others (Nelson 2010; Wei, 2010; Svendsen and Mangerud, 1997; Snyder et al., 2000; Thomas and Briner, 2009). In the LH-4 varve record periods of cool summer temperatures can be defined from AD 1400-1450's, AD 1550's-1580's, AD 1790's-1850's and AD 1950's-1980's. The earliest cool period relates to low temperatures recorded at Kongressvatnet and the final cool period is synchronous to a significant cooling trend in the Svalbard Airport annual air temperature record (D'Andrea et al., 2012; Førland et al., 2011).

In order to place the Linnédalen climate trends projected from the LH-4 varved sediment record into regional context these trends must be compared to Late Holocene North Atlantic and Arctic climate records. These proxy-based records, shown in Figure 27, are the Kongressvatnet summer temperature reconstruction (D'Andrea et al., 2012), the Lomonosovfonna, Svalbard ice core oxygen isotope record (Isaksson et al., 2005), the GISP2 ice core oxygen isotope record (Grootes and Stuvier, 1997), Northern Hemisphere Volcanic Forcing (Briffa et al., 1998), a tree-ring based NAO index reconstruction (Trouet et al., 2009) and solar insolation at 60°N (Berger and Loutre, 1991).

The oxygen isotope curve from the Lomonosovfonna Ice Core is a winter temperature proxy based on the temperature dependent fractionation of oxygen isotopes during the precipitation of snow, which is preserved in the ice cap through time (Isaksson et al., 2005). This curve, shown in purple in Figure 27, is characterized by a gradual decline from AD 1400 to 1900 and then a spike from 1900 to the present (Isaksson et al., 2005). The long decline is dominated by low-frequency oscillation (Isaksson et al., 2005). A linear regression between $\delta^{18}O$ values and varve thickness based on 1, 5 and 11 year averages did not result in R^2 values above 0.1. The low correlation is due to the fact that $\delta^{18}O$ is a winter temperature proxy and the LH-4 varve record is a summer temperature proxy (Isaksson et al., 2005). One similarity that can be drawn is the enrichment in $\delta^{18}O$ values at Lomonosovfonna interpreted as the end of the Little Ice Age occurs just after the 1850's-1870's warm period defined from the LH-4 varve record. Therefore a possible interpretation of the 1850's-1870's warming in Linnédalen could be that it marks the initial stages of Little Ice Age termination in Linnédalen.

The oxygen isotope curve from the GISP 2 ice core, shown in blue in Figure 27, is also a winter temperature proxy (Grootes and Stuiver, 1997). This proxy record shows high variability since AD 1379 with no dominant trends. Overall, there is not a strong correlation between the GISP2 $\delta^{18}O$ values and the climate picture developed from the LH-4 varve record

Summer temperature anomaly in the northern hemisphere related to volcanic forcing is shown in dark red in Figure 27. Volcanic forcing can have a major effect on climate of the Northern Hemisphere and has been considered a potential factor in the onset of the Little Ice Age (Miller et al., 2012). Overall the reconstructed temperature anomaly does not correspond well to the LH-4 climate picture. The lowest summer temperature anomaly corresponds to a significant decrease in varve thickness centered on AD 1820. Other correlation between low summer temperature anomaly

and decreased varve thickness is not evident throughout the LH-4 varve record. If the LH-4 record extended to pre-LIA there may be good correlation between the LH-4 climate signal and the volcanic forcing that may have triggered the LIA (Miller et al., 2012).

NAO index reconstructed from tree-rings is shown in green in Figure 27. There is very strong correlation between NAO index and climate conditions in Linnédalen reconstructed in this study. Each cold period defined in the reconstruction relates to a period of negative NAO index. The same holds for the warm periods which correspond to the increases and maxima in the reconstructed NAO index. The strong correlation between NAO and climate conditions in Linnédalen is due to the strong effect of NAO on the WSC and the climate of western Spitsbergen (Schlichtholz and Goszczko, 2006; Rasmussen and Kohler, 2007). The positive mode of the NAO results in warm temperatures in the WSC (Schlichtholz and Goszczko, 2006). This warm ocean water hugs the western coast of Spitsbergen and a finger of the WSC reaches into Isfjorden surrounding Linnédalen (Rasmussen et al., 2012). The warmer water results in warmer climate conditions on West Spitsbergen (Schlichtholz and Goszczko, 2006; Rasmussen et al., 2012). Research by Rasmussen and Kohler (2007) on glaciers in northwestern Spitsbergen has shown good correlation between glacier mass balance and NAO index since 1948. This indicates that the warm temperatures that result from positive NAO mode are substantial enough to affect glacier mass balance. It is likely that the same relationship is evident for Linnébreen, due to its similarities to the glaciers examined in the study. The strong correlation between LH-4 varve thickness and NAO index throughout the Late Holocene suggests that this relationship exists as far back as AD 1379.

Northern Hemisphere solar insolation, shown in red in Figure 27, has been steadily decreasing over the Holocene with a slight leveling of the curve during the Late Holocene (Berger and Loutre, 1991). This long term trend of decreasing solar insolation is not evident in the LH-4 climate signal due to shortness of the 600+ interval it covers. Overall, climate conditions in the Arctic during the Holocene follow the gradual decline in solar insolation (Larsen et al., 2012). However during the Late Holocene the observed non-linear response of Arctic climate conditions to changes in insolation is due to the complex interactions between insolation, feedback mechanisms and additional climate forcing agents (Larsen et al., 2012). In Linnédalen and all of western Spitsbergen, patterns of ocean and atmospheric circulation related to many factors including sea surface temperatures and sea ice extent have a stronger impact on short term changes in climate conditions than insolation (Rasmussen et al., 2012, Schlichtholz and Goszczko, 2006; Piechura and Walczowski, 2009; Walczowski and Piechura, 2011).

Conclusion

While previous analyses of the Linnévatnet sediment record have focused on reconstructing long-term trends in glacier activity and climatic conditions in Linnédalen, this study reconstructs the past 600 years of climate variability in Linnédalen on decadal to century scale (Svendsen and Mangerud, 1997; Snyder et al., 2000). This reconstruction, based on the physical characteristics of core LH-4, projects paleoclimate conditions in Linnédalen for the last 600 years. This high-resolution reconstruction was established by developing a plutonium-verified varve chronology and using varve thickness and grains size as the primary climate proxies. The accuracy of these proxies was determined through an understanding of the Linnédalen proglacial environment and comparison with proximal paleoclimate reconstructions derived from other proxies. The varve chronology has an uncertainty of 4% but is one of the highest resolution age models developed from the Linnévatnet sediment record.

Through the interpretation of varve thickness and grain size variations along core LH-4 and comparisons between the LH-4 varve record and other Svalbard paleoclimate reconstructions four periods of warm summer temperatures and four periods of cool summer temperatures were projected in the past 600 years. The warm periods, defined as AD pre-1379 to late 1390's, AD 1760's-1790's, AD 1850's to AD 1870's, and AD 1980's-present, relate to either steady increases in LH-4 varve thickness or sustained intervals of above average varve thickness. The cool periods, defined as AD 1400-1450's, AD 1550's-1580's, AD 1790's-1850's and AD 1950's-1980's, relate to either steady decreases in LH-4 varve thickness or sustained intervals of below average varve thickness.

The Late Holocene paleoclimate picture of Linnédalen developed in this study correlates well with the summer temperature Kongressvatnet reconstruction by D'Andrea et al., (2012) and NAO index reconstructed from tree-rings by Trouet et al. (2009). The alignment with the Kongressvatnet record served to both confirm the interpretation of climate proxies in the Linnévatnet sediment record and define two of the warmest periods in Linnédalen during the Late Holocene. The correlation with NAO index supports work by others that suggest the WSC and NAO mode have a major influence on the climate of West Spitsbergen (Schlichtholz and Goszczko, 2006; Rasmussen et al., 2012).

Future Work

Overall, the sediment cores analyzed in this study allowed for the thorough analysis of climate proxies and the establishment of an accurate plutonium-verified varve chronology. The paleoclimate picture presented in this study could be extended at least another 1,000 years through further analysis of core LH-Long. Additionally, future work developing the understanding of how both summer temperature and precipitation affect the sediment record at site H would allow for a more accurate reconstruction to be developed. Finally, the uncertainties in both the varve chronology and varve thickness measurements could be lessened with the collection of a more proximal core that spans the same time interval as core LH-4. Correlation between LH-4 and a proximal core would

allow for the sub-annual layering, seen more clearly in the proximal core, to be related to laminations in LH-4. With this two-core approach sub-annual layers could be more accurately identified improving the age model and varve thickness measurements.

References

Arnold, M., 2009, Sedimentation in High-Arctic Lake, Linnèvatnet, Svalbard: A Modern Process Study Using Sediment Traps: Bates College Unpublished Thesis.

Axford, Y., Briner, J., Cooke, C., Francis, D., Michelutti, N., Miller, G., Smol, J., Thomas, E., Wilson, C., Wolfe, A., 2009, Recent changes in a remote Arctic lake are unique within the past 200,000 years: PNAS Early Edition, p. 1-4.

Berger A. and Loutre M.F., 1991. Insolation values for the climate of the last 10 million years. Quaternary Science Reviews: Vol. 10 No. 4, pp. 297-317, 1991.

Bradley, R., Hughes, M. K., Diaz, H. F., 2003, Climate in Medieval Time: Science, v. 302, p. 404-405.

Boyum, A., & Kjensmo, J., 1978, Physiography of Lake Linnevatnet, Western Spitsbergen. In Proceedings: 20th Congress, Internationale Vereinigung fur Theoretische und Angewandte Limnologie.

Briffa, K. R., Schweingruber, F.H., Jones, P. D., Osborn, T. J., Shiyatov, S. G., Vaganov, E. A., 1998, Northern Hemisphere Temperature Reconstructions. IGBP PAGES/World Data Center-A for PaleoclimatologyData Contribution Series #98-022. NOAA/NGDC Paleoclimatology Program, Boulder CO, USA

D'Andrea, W. J., Vaillencourt, D., Balascio, N. L., Werner, A., Roof, S. R., Retelle, M., Bradley, R. S. ,2012, Mild Little Ice Age and unprecedented recent warmth in an 1800 year lake sediment record from Svalbard: Geology, v. 40, p. 1007-1010.

Denton, G.H. and W. Karlen, 1977,Holocene Glacial and Tree Line Variations in the White River Valley and Skolai Pass, Alaska and Yukon Territory: Quaternary Research, v. 7, p. 63-111.

DeWet, G., 2013, Holocene Climate Variability Reconstructed From A Lake Sediment Record In SE Greenland, Arctic Workshop Presentation.

Farnsworth, L., 2013, personal communication.

Forland, E. J., Benestad, R., Hanssen-Bauer, I., Haugen, J. E., Skaugen, T. E., 2011, Temperature and precipitation development at Svalbard 1900-2100: Advances in Meteorology, v. 2011, p 1-14.

French, H. M., & Slaymaker, O., 1997, Canada's cold environments. McGill-Queen's University Press.

Ingolfsson, O. "Outline of the Physical Geography and Geology of Svalbard." 2006.

Grootes, P. M., Stuiver, M., 1997, GISP2 Oxygen Isotope Data. doi:10.1594/PANGAEA.56094

IPCC, International Panel on Climate Change, 2007, Climate Change 2007: Synthesis Report, Edited by A. Reisinger R.K. Pauchari. IPCC Fourth Assessment Report, 2007. Geneva, Switzerland, 2007.

Isakkson, E., Kohler, J., Pohjola, V., Moore, J., Igarashi, M., Karlof, L., Martma, T., Meijer, H., Motoyama, H., Vaikmae, R., van de Wal, R. S. W., 2005, Two ice core d18O records from Svalbard illustrating climate and sea-ice variability over the last 400 years: The Holocene, v. 15, p. 501-509.

Kattsov, V., Killen, E., Cattle, H., Christensen, J., Drange, H., Hanssen-Bauer, 1.,Johannesen, T., Karol, 1., Riiisanen, J., Svensson, G., Vavulin, S., 2005, Future climate change: Modeling and scenarios for the Arctic: Arctic Climate Impact Assessment Scientific Report.

Ketterer, M.E., Hafer, K.M., Jones, V.J., and Appleby, P.G., 2004, Rapid dating of recent sediments in Loch Ness: inductively coupled plasma mass spectrometric measurements of global fallout plutonium: Science of the Total Environment, v. 322, p. 221–229.

Hardy, D. R., Bradley, R. S., Zolitschka, B., 1996, The climatic signal in varved sediments from Lake C2, northern Ellesmere Island, Canada: Journal of Paleolimnology, v. 16, p. 227-238.

Hughen, K. A., Overpeck, J. T., Anderson, R. F., 2000, Recent warming in a 500-year paleotemperature record from varved sediments, Upper Soper Lake, Baffin Island, Canada. The Holocene, v. 10, p. 9-19.

Humlum, O., Eberling, B., Hormes, A., Fjordheim, K., Hansen, O.H., and Heinemeier, J., 2005, Late-Holocene glacier growth in Svalbard, documented by subglacial relict vegetation and living soil microbes: The Holocene, v. 15, p. 396-407.

Larsen, D. J., Miller, G. H., Geirsdottir, A., Olafsdottir, S., 2012, Non-linear Holocene climate evolution in the North Atlantic: a high-resolution, multi-proxy record of glacier activity and environmental change from Hvítárvatn, central Iceland: Quaternary Science Reviews, v. 39, p. 14-25.

Leeman, A. and Niessen, F. 1994: Holocene glacial activity and climatic variations in the Swiss Alps: reconstructing a continuous record from proglacial lake sediments: The Holocene, v.4, p. 259-68.

Leonard, E. M., Reasoner, M. A., 1999, A continuous Holocene glacial record inferred from proglacial lake sediments in Banff National Park, Alberta, Canada: Quaternary Research, v. 51, p. 1-13.

Leonard, E. M., 1997, The relationship between glacial activity and sediment production: evidence from a 4450-year varve record of neoglcial sedimentation in Hector Lake, Alberta, Canada: Journal of Paleolimnology, v. 17, p. 319-330.

Lowell, T.V., 2000, As climate changes, so do glaciers: Proceedings of the National Academy of Sciences - PNAS, v. 97, p. 1351-1354.

Lund, D., Lunch-Stieglitz, J., Curry, W., 2006, Gulf Stream density structure and transport during the past millennium: Nature, v.444, 601--604.

Mangerud, J., Svendsen, J.I., 1990, Deglaciation chronology inferred from marine sediments in a proglacial lake basin, western Spitsbergen, Svalbard: Boreas, v. 19, p. 249-272.

Mann, M., Bradley, R., Hughes, M., 1998, Global-scale temperature patterns and climate forcing over the past six centuries: Nature, v. 392, 779-787.

McKay, N., 2005, Characterization of Climatic Influences on Modern Sedimentation in an Arctic Lake, Svalbard, Norway: Northern Arizona University Unpublished Thesis.

Miller, G. H., Geirsdottir, A., Zhong, Y., Larsen, D. J., Otto-Bliesner, B., Holland, M. M., Bailey, D. A., Refsnider, K. A., Lehman, S. J., Southon, J. R., Anderson, C., Bjornsson, H., Thordarson, T., 2012, Abrupt onset of the Little Ice Age triggered by volcanism and sustained by sea-ice/ocean feedbacks: Geophysical Research Letters, v. 39, p. 1-5.

Motley, J., 2006, Sedimentation in Linnevatnet, Svalbard, during 2004-2005, a modern process study using sediment traps: Bates College Unpublished Thesis.

Nelson, A., 2010, A Varved Sediment Aanalysis of 1,000 Years of Climate Change: Linnevatnet,Svalbard: Bates College Unpublished Thesis.

Nereson, A., 2010, Sedimentation rates in the distal basin ofArctic proglacial lake Linnevatnet, Western Spitsbergen, Svalbard: Evidence from radioactive Cesium-137,Undergraduate Capstone Report, Department of Geology, Macalester College.

Nordli, P.Ø., Kohler, J., 2004, The early 20th Century Warming Daily observations at Green Harbour, Gronfjorden, Spitsbergen: Rapport Kilma 12/03.

Obermeyer, D., 2013, Personal communication at Arctic Workshop at UMASS Amherst.

Ojala, A. E. K., Francus, P., Zolitschka, B., Besonen, M., Lamoureux, S. F., 2012, Characteristics of sedimentary varve chronologies – A review: Quaternary Science Reviews, v. 43, p. 45-60.

Osleger, D. A., Hayvaert, A. C., Stoner, J. S., Verosub, K. L., 2009, Lacustrine turbidites as indicators of Holocene storminess and climate: Lake Tahoe, California and Nevada: Journal of Paleolimnology, v. 42, p. 103-122.

Perreault, L., 2006, Mineralogical Analysis of Primary and Secondary Source Sediments to Linnevatnet, Spitsbergen, Svalbard: Unpublished Bates College Thesis.

Piechura, J., Walczowski, W., 2009, Warming of the West Spitsbergen Current and sea ice north of Svalbard: Oceanologia, v. 51, p. 147-164.

Pompeani, D., Abbott, M., Ortiz, J., Bain, D., Smith, S., 2009, A 360 year varve-based climate reconstruction from Linnevatnet on western Svalbard: Unpublished University of Pittsburgh Paper.

Pratt, E., 2006, Characterization and Calibration of Lamination Stratigraphy of Cores Recovered from Lake Linne, Svalbard, Norway: Unpublished Mount Holyoke College Independent Study.

Rasmussen, T.L., Forwick, M., and Mackensen, A., 2012, Reconstruction of inflow of Atlantic Water to Isfjorden, Svalbard during the Holocene: Correlation to climate and seasonality: Marine Micropaleontology, v. 94–95, p. 80-90, doi: 10.1016/j.marmicro.2012.06.008.

Rasmussen, L. A., Kohler, K., 2007, Mass balance of three Svalbard glaciers reconstructed back to 1948: Polar Research, v. 26, p. 168-174.

Retelle, M. J., 2013, personal communication.

Schlichtholz, P., Goszczko, I., 2006, Interannual variability of the Atlantic water layer in the West Spitsbergen Current at 76.5N in summer 1991–2003: Deep Sea Research I, v. 53, p. 608-626.

Smith, N.D., and Ashley, G., 1985, Proglacial lacustrine environments. Ch. 4, in Glacial

Sedimentary Environments, eds. Ashley, G., Shaw, J., and Smith, N.D.; S.E.P.M. short course no. 16, p. 135-215.

Snyder, J.A., Werner, A., and Miller, G.H., 2000, Holocene cirque glacier activity in western Spitsbergen, Svalbard: sediment records from proglacial Linnevatnet, Holocene, v.10, 555-563.

Svendsen, J.I., Landvik, J.Y., Mangerud, J., and Miller, G.H., 1987, Postglacial marine and lacustrine sediments in Lake Linnévatnet , Svalbard: Polar Research, v. 5, p. 281-283.

Svendsen, J. I., Mangerud, J., & Miller, G. H.,1989, Denudation rates in the Arctic estimated from lake sediments on Spitsbergen, Svalbard: Palaeogeography, Palaeoclimatology, Palaeoecology, v. 76, p. 153-168.

Svendsen, J.1., and Mangerud, J., 1997, Holocene glacial and climatic variations on Spitsbergen, Svalbard: The Holocene, v. 7, 45-57.

Thompson, L.G., Mosley-Thompson, W., Dansgaard, W., Grootes, P. M., 1986, The Little Ice Age as Recorded in the Stratigraphy of the Tropical Quelccaya Ice Cap: Science, v. 234, p. 361-364.

Thomas, E. K., Briner, J. P., 2009, Climate of the past millennium inferred from varved proglacial lake sediments on northeast Baffin Island, Arctic Canada: Journal of Paleolimnology, v. 41, p. 209-224.

Trouet, V., Esper, J., Graham, N. E., Baker, A., Scourse, J. D., Frank, D. C., 2009, Persistent Positive North Atlantic Oscillation Mode Dominated the Medieval Climate Anomaly: Science, v. 324, p. 78-80.

Walczowski, W., Piechura, J., 2011, Influence of the West Spitsbergen Current on the local climate: International Journal of Climatology, v. 31, p. 1088-1093.

Wanner, H., Beer, J., Biitikofer, J., Crowley, T., Cubasch, U., Fliickiger, J., Goosse, H.,Gfosjean, M., Joos, F., Kaplan, J., Kiittel, M., Milller, S., Prentice, 1., Solomina, 0., Stocker, T., Tarasov, P., Wagner, M., Widmann, M., 2008, Mid- to Late Holocene climate change: an overview: Quaternary Science Reviews, v. 27, 1791-1828.

Wei, J., 2010, Analysis of Varved Sediment and Weather Relationships in Lake Linnè, Svalbard: Tufts University Undergraduate Thesis.

Werner, A., 1993, Holocene moraine chronology, Spitsbergen, Svalbard: lichenometric evidence for multiple Neoglacial advances in the Arctic: The Holocene, v. 3, p 123-137.

Wood, R. M., Woo, G., 1987, The historical seismicity of the Norwegian continental shelf: ELOCS Report 2-1, p. 1-53.